MATHEMATICS OF COMPUTATION
Volume 85, Number 297, January 2016, Pages 1–33
http://dx.doi.org/10.1090/mcom/2980
Article electronically published on June 8, 2015

# A MIXED FINITE ELEMENT METHOD FOR DARCY'S EQUATIONS WITH PRESSURE DEPENDENT POROSITY

GABRIEL N. GATICA, RICARDO RUIZ-BAIER, AND GIORDANO TIERRA

Abstract. In this work we develop the a priori and a posteriori error analyses of a mixed finite element method for Darcy's equations with porosity depending exponentially on the pressure. A simple change of variable for this unknown allows us to transform the original nonlinear problem into a linear one whose dual-mixed variational formulation falls into the frameworks of the generalized linear saddle point problems and the fixed point equations satisfied by an affine mapping. According to the latter, we are able to show the well-posedness of both the continuous and discrete schemes, as well as the associated Cea estimate, by simply applying a suitable combination of the classical Babuška-Brezzi theory and the Banach fixed point theorem. In particular, given any integer $k \geq 0$, the stability of the Galerkin scheme is guaranteed by employing Raviart-Thomas elements of order $k$ for the velocity, piecewise polynomials of degree $k$ for the pressure, and continuous piecewise polynomials of degree $k+1$ for an additional Lagrange multiplier given by the trace of the pressure on the Neumann boundary. Note that the two ways of writing the continuous formulation suggest accordingly two different methods for solving the discrete schemes. Next, we derive a reliable and efficient residual-based a posteriori error estimator for this problem. The global inf-sup condition satisfied by the continuous formulation, Helmholtz decompositions, and the local approximation properties of the Raviart-Thomas and Clément interpolation operators are the main tools for proving the reliability. In turn, inverse and discrete inequalities, and the localization technique based on triangle-bubble and edge-bubble functions are utilized to show the efficiency. Finally, several numerical results illustrating the good performance of both methods, confirming the aforementioned properties of the estimator, and showing the behaviour of the associated adaptive algorithm, are reported.

## 1. Introduction

The understanding and accurate rendering of fluid velocities and pressure of the porous medium is of key importance in diverse applications covering, for instance, groundwater pollution, mezoscale blood flows, filters design, enhanced oil recovery,

Received by the editor February 18, 2014 and, in revised form, June 11, 2014 and July 21, 2014.

2010 *Mathematics Subject Classification.* Primary 65N15, 65N30, 74F10, 74S05.

The work of the first author was partially supported by CONICYT-Chile through BASAL project CMM, Universidad de Chile, and project Anillo ACT1118 (ANANUM); by the ministry of Education through the project REDOC.CTA of the Graduate School, Universidad de Concepción; and by Centro de Investigación en Ingeniería Matemática (CI$^2$MA), Universidad de Concepción.

The work of the second author was partially supported by the University of Lausanne and by the Swiss National Science Foundation through grant PPOOP2-144922.

The work of the third author was partially supported by the Ministry of Education, Youth and Sports of the Czech Republic through the ERC-CZ project LL1202. Part of this research was developed while this author was visiting CI$^2$MA during the last three weeks of January 2014.

©2015 American Mathematical Society



Licensed to University of Oxford. Prepared on Fri Oct 16 07:02:22 EDT 2015 for download from IP 129.67.185.217.
License or copyright restrictions may apply to redistribution; see http://www.ams.org/journal-terms-of-use

carbon dioxide sequestration, and many others. In case of negligible relaxation time, and under relatively small permeability, it is possible to model the fluid flow in rigid porous media employing the well-known Darcy's law [22] which relates pressure gradient of the fully saturated porous medium with the velocity of the viscous incompressible fluid (volumetric flux). This model can be regarded as a starting point in the study of more involved and complex flow phenomena, and a myriad of numerical methods in different flavors and with increasingly appealing features has emerged in the past few decades. In particular, the development of suitable numerical methods for solving the Stokes-Darcy and related coupled problems, including porous media with cracks, the incorporation of the Brinkman equation in the model, and linear as well as nonlinear behaviors, has become a very active research area during the last decade (see, e.g., [13], [23], [25], [26], [31], [32], [37], [48], [55] and the references therein).

Our objective in this paper is to propose, analyze and implement a family of mixed finite element methods targeted to simulate the more general case where the porosity of the medium may depend explicitly (and exponentially) on the pressure, turning the classical Darcy equations into a nonlinear system of equations. Indeed, the fact that the viscosity of a fluid could depend on pressure is very well established. For instance, as early as 1893, Barus was aware of these dependences [11], suggesting an exponential dependence of the viscosity on the pressure, i.e., $\mu(p) = \mu_0\, e^{\beta p}$, where $\mu_0 > 0$ and $\beta \geq 0$ are constants, with $\mu_0$ having the dimension of viscosity and $\beta$ the dimension inverse to that of the pressure. This pressure-dependent viscosity would lead to a drag coefficient $\alpha(p)$ of the form $\alpha(p) = \alpha_0\, e^{\beta p}, \quad \alpha_0 \geq 0$. We refer to [50] for a generalization of the classical Brinkman equation considering the dependence on pressure of the viscosity and the drag coefficient.

More precisely, in this work we are interested in the case in which the dissipation due to the drag at the pores is much larger than the dissipation due to the shear in the bulk fluid. Such a specific problem has been introduced in [47] and some attempts to approximate the system have been proposed recently. In fact, in [6] the authors present optimal error estimates for a spectral discretization of this system which takes into account the axisymmetry of the domain and of the flow. On the other hand, in [33] the authors consider first the simplified model in which the exponential law defining the porosity is truncated above and below by positive constants, whose corresponding solvability and regularity analysis was previously developed in [6], and propose a primal finite element scheme with polynomial approximations of degrees $k-1$ and $k$ for velocity and pressure, respectively. Then, the case of a fully exponential porosity is analyzed in the second part of [33], where, under the heuristic assumption that the resulting model has at least one solution, a suitable change of variables involving only the pressure allows us to split the problem into two consecutive linear systems, which are discretized by slight variants of the method from the first part. Numerical results show the good performance of this approach. However, further regularity on the right-hand side datum needs to be assumed in order to derive a Robin-type boundary condition yielding the well-posedness of the continuous formulation. More recently, a strategy based on a posteriori error analysis and leading to an automatic identification of the subdomain where the pressure presents high variations, has been proposed in [2]. In this way, the iterative method needed to handle the nonlinear term is only applied in that region whereas the permeability is approximated by a constant in the remaining

Licensed to University of Oxford. Prepared on Fri Oct 16 07:02:22 EDT 2015 for download from IP 129.67.185.217.
License or copyright restrictions may apply to redistribution; see http://www.ams.org/journal-terms-of-use

part. The resulting simplified model is then discretized in [2] by spectral elements as in [6], [7], and [21]. Other related works include [41], [42], and [18], where least squares and variational multiscale discretizations of Darcy's equations with pressure dependent viscosity have been extensively studied, and those referring to the nonlinear Darcy system given by the well-known Forchheimer model (see, e.g., [35], [44], and [45]).

Here we also consider the Darcy model with a fully exponential porosity from the second part of [33], assume again the heuristic hypothesis concerning the existence of a solution, and apply the same change of variables employed there, but instead of a primal method, we opt for using the dual-mixed approach. As a consequence, the mixed boundary conditions arising from the transformation become readily employable and hence there is no need of additional regularity on the data nor of deriving any other boundary condition. In addition, the velocity unknowns of both problems coincide and the original pressure is recovered by a simple postprocessing formula depending only on the pressure of the transformed model. Moreover, the resulting dual-mixed variational formulation can be written as a generalized linear saddle point problem, and also as a fixed point equation satisfied by an affine mapping whose linear component is given by the solution of a usual linear saddle point problem. The first way of writing the continuous formulation emphasizes the fact that in this case the change of variables transforms the original nonlinear problem into a single linear one, whereas the second way allows us to show the well-posedness of both the continuous and discrete problems, as well as the associated Cea estimate, by simply combining the classical Babuška-Brezzi theory with the Banach fixed point Theorem. In addition, the above suggests two different numerical methods for the Galerkin scheme, namely a fixed point iterative procedure solving symmetric systems each time, and a direct solver of a single nonsymmetric system.

Next, we derive a reliable and efficient residual-based a posteriori error estimator for the transformed problem and show the satisfactory performance of our method by means of several numerical tests. We remark that the application of adaptive algorithms based on a posteriori error estimates aims to identify the regions with singularities or high gradients, so that further refinements are applied there at each stage, thus improving the convergence behavior of the Galerkin solutions of linear and nonlinear boundary value problems. The global estimator is normally represented by a quantity $\boldsymbol{\theta}$ depending on local estimators $\theta_T$ defined on each element $T$ of a given triangulation of the domain. Then, $\boldsymbol{\theta}$ is said to be reliable (resp. efficient) if there exists $C_{\mathtt{rel}} > 0$ (resp. $C_{\mathtt{eff}} > 0$), independent of the meshsizes, such that

$$C_{\mathtt{eff}}\,\boldsymbol{\theta} + \text{h.o.t.} \;\leq\; \|\text{error}\| \;\leq\; C_{\mathtt{rel}}\,\boldsymbol{\theta} + \text{h.o.t.}\,,$$

where h.o.t. is a generic expression denoting one or several terms of higher order. While the list of references on a posteriori error analysis for mixed formulations of linear and nonlinear problems is nowadays quite extensive, which includes several important contributions in recent years, most of the main ideas and associated techniques employed can be found in [3], [4], [14], [17], [30], [52], [54], and the references therein. In particular, the first corresponding results for elliptic partial differential equations of second order, which consider a posteriori error estimators of explicit residual type, the solution of local problems, and the eventual derivation of reliability and efficiency properties, among other issues, go back to [52], [4], [14] and [17]. To this respect, we just mention here that the main tools for reliability and efficiency, which will also be employed below in Section 5, include Helmholtz decompositions, the localization technique based on bubble functions, discrete trace and inverse inequalities, and the approximation properties of the Clément interpolant.

Licensed to University of Oxford. Prepared on Fri Oct 16 07:02:22 EDT 2015 for download from IP 129.67.185.217.
License or copyright restrictions may apply to redistribution; see http://www.ams.org/journal-terms-of-use

The rest of this paper is organized as follows. We end this section with some notations to be used below. Section 2 introduces the nonlinear Darcy problem, which after a change of variables is written in mixed form. In Section 3 we derive the variational mixed formulation of the problem and establish its unique solvability using a fixed point argument. Section 4 is concerned with the construction and well-posedness analysis of a general Galerkin scheme for the discrete approximation of the modified problem, and we provide examples of finite element subspaces satisfying the underlying assumptions. A detailed residual-based a posteriori error analysis is carried out in Section 5, written specifically for the two-dimensional case. Finally, several examples are provided in Section 6, illustrating the accuracy of the aforementioned numerical methods, confirming the reliability and efficiency of the a posteriori error estimator previously derived, and showing the good performance of the associated adaptive algorithm.

In what follows we utilize standard simplified terminology for Sobolev spaces and norms. In particular, if $\mathcal{O} \subseteq \mathbb{R}^d$ ($d \in \{2,3\}$) is a domain, $\mathcal{S} \subseteq \mathbb{R}^d$ is a Lipschitz curve or surface, and $r \in \mathbb{R}$, we define

$$\boldsymbol{H}^r(\mathcal{O}) := [H^r(\mathcal{O})]^d \quad \text{and} \quad \boldsymbol{H}^r(\mathcal{S}) := [H^r(\mathcal{S})]^d .$$

However, when $r = 0$ we usually write $\boldsymbol{L}^2(\mathcal{O})$ and $\boldsymbol{L}^2(\mathcal{S})$ instead of $\boldsymbol{H}^0(\mathcal{O})$ and $\boldsymbol{H}^0(\mathcal{S})$, respectively. The corresponding norms are denoted by $\|\cdot\|_{r,\mathcal{O}}$ (for $H^r(\mathcal{O})$ and $\boldsymbol{H}^r(\mathcal{O})$) and $\|\cdot\|_{r,\mathcal{S}}$ (for $H^r(\mathcal{S})$ and $\boldsymbol{H}^r(\mathcal{S})$). In general, given any Hilbert space $H$, we use $\boldsymbol{H}$ to denote $H^d$. In turn, the Hilbert space $\boldsymbol{H}(\mathrm{div};\mathcal{O}) := \big\{\boldsymbol{w} \in \boldsymbol{L}^2(\mathcal{O}) : \mathrm{div}\,\boldsymbol{w} \in L^2(\mathcal{O})\big\}$, whose norm is given by

$$\|\boldsymbol{w}\|_{\mathrm{div},\mathcal{O}} := \Big\{\|\boldsymbol{w}\|_{0,\mathcal{O}}^2 + \|\mathrm{div}\,\boldsymbol{w}\|_{0,\mathcal{O}}^2\Big\}^{1/2} \qquad \forall\, \boldsymbol{w} \in \boldsymbol{H}(\mathrm{div};\mathcal{O})\,, \tag{1.1}$$

is standard in the realm of mixed problems (see [15]). Finally, we employ $\mathbf{0}$ to denote a generic null vector (including the null functional and operator), and use $C$ and $c$, with or without subscripts, bars, tildes or hats, to denote generic constants independent of the discretization parameters, which may take different values at different places.

## 2. The model problem

Let $\Omega \subseteq \mathbb{R}^d$ be a bounded domain ($d \in \{2,3\}$) with Lipschitz-boundary. The boundary of this domain is divided in two portions $\Gamma_D$ and $\Gamma_N$, such that $\Gamma_D \cap \Gamma_N = \emptyset$ and $|\Gamma_D| > 0$, on which different types of boundary conditions will be imposed. We are interested in the model governing the flow of an incompressible fluid through a porous solid that can be derived within the context of mixtures, following e.g. [47]. The Cauchy stress $\mathbb{T}$ of the fluid is given by $\mathbb{T} = -P\,\mathbb{I} + \mu\,\mathbb{D}$, where $P$ denotes the pressure of the fluid, $\mathbb{I}$ is the identity matrix of $\mathbb{R}^d$, $-P\,\mathbb{I}$ is the indeterminate part of the stress due to the constraint of incompressibility, $\mu$ is the viscosity and $\mathbb{D}$ denotes the symmetric part of the velocity gradient, i.e., $\mathbb{D} = \frac{1}{2}\Big(\nabla \boldsymbol{U} + (\nabla \boldsymbol{U})^t\Big)$, where $\boldsymbol{U}$ is the velocity of the fluid. The balance of linear momentum for the fluid, is given by

$$\rho\,\frac{\partial \boldsymbol{U}}{\partial t} - \mathbf{div}\,\mathbb{T} + \mathbb{F} = \rho\,\boldsymbol{f},$$

where $\mathbf{div}$ is the usual divergence operator div acting row-wise, $\mathbb{F}$ is the interaction between the solid and the fluid, namely the frictional resistance at the pores of the solid on the fluid that is flowing. We shall assume that virtual mass effects, lift,

Licensed to University of Oxford. Prepared on Fri Oct 16 07:02:22 EDT 2015 for download from IP 129.67.185.217.
License or copyright restrictions may apply to redistribution; see http://www.ams.org/journal-terms-of-use

and Basset forces can be neglected so that the only interaction mechanism is due to the drag, that is $\mathbb{F} = \alpha(P)\,\boldsymbol{U}$, where $\alpha$ is the pressure dependent permeability of the medium. Moreover, if the dissipation due to the drag at the pores is much larger than the dissipation due to the shear in the bulk fluid, it is reasonable to simplify the Cauchy stress to $\mathbb{T} = -P\,\mathbb{I}$. We refer the reader to [51] for a thermodynamic basis for the derivation of models for flows through porous media and their generalizations. It follows from the previous relations, on neglecting the inertial term, that the appropriate governing equations supplemented by mixed boundary conditions are

$$\begin{aligned} \alpha(P)\,\boldsymbol{U} + \nabla P = \boldsymbol{f} \quad \text{in} \quad \Omega\,, \quad \operatorname{div}\boldsymbol{U} = 0 \quad \text{in} \quad \Omega\,, \\ P = 0 \quad \text{on} \quad \Gamma_D\,, \quad \boldsymbol{U}\cdot\boldsymbol{\nu} = g \quad \text{on} \quad \Gamma_N\,, \end{aligned} \tag{2.1}$$

where $\boldsymbol{f} \in \boldsymbol{L}^2(\Omega)$ and $g \in H_{00}^{-1/2}(\Gamma_N)$ (see below for a definition of this space). Throughout this paper we also assume that $\alpha$ depends exponentially on $P$, that is, there exist constants $\alpha_0,\, \gamma > 0$ such that

$$\alpha(s) = \alpha_0\, e^{\gamma\, s} \qquad \forall\, s \in \mathbb{R}\,.$$

Hence, we rewrite the first equation of (2.1) as:

$$\boldsymbol{U} = \frac{1}{\alpha(P)}\,(\boldsymbol{f} - \nabla P) = \frac{1}{\alpha_0}\,(e^{-\gamma P}\,\boldsymbol{f} - e^{-\gamma P}\,\nabla P) = \frac{1}{\alpha_0}\,\left(e^{-\gamma P}\,\boldsymbol{f} + \frac{1}{\gamma}\,\nabla(e^{-\gamma P})\right),$$

so that, assuming heuristically that (2.1) has at least one solution, and defining the new unknowns

$$\boldsymbol{u} := \boldsymbol{U} \quad \text{and} \quad p := e^{-\gamma P} - 1 \quad \text{in } \Omega\,,$$

we can recast (2.1) in the form

$$\begin{aligned} \boldsymbol{u} = \frac{1}{\alpha_0}\,(p+1)\,\boldsymbol{f} + \frac{1}{\alpha_0\,\gamma}\,\nabla p \quad \text{in} \quad \Omega\,, \quad \operatorname{div}\boldsymbol{u} = 0 \quad \text{in} \quad \Omega\,, \\ p = 0 \quad \text{on} \quad \Gamma_D\,, \quad \boldsymbol{u}\cdot\boldsymbol{\nu} = g \quad \text{on} \quad \Gamma_N\,, \end{aligned} \tag{2.2}$$

Furthermore, we recall that the Sobolev space to which the Neumann datum $g$ belongs, that is $H_{00}^{-1/2}(\Gamma_N)$, is the dual of $H_{00}^{1/2}(\Gamma_N)$, where

$$H_{00}^{1/2}(\Gamma_N) := \left\{ v|_{\Gamma_N} : \quad v \in H^1(\Omega)\,, \quad v = 0 \quad \text{on} \quad \Gamma_D \right\}.$$

Equivalently, we can define

$$H_{00}^{1/2}(\Gamma_N) := \left\{ \xi \in H^{1/2}(\Gamma_N) : \quad E_{N,0}(\xi) \in H^{1/2}(\partial\Omega) \right\},$$

which is endowed with the norm

$$\|\xi\|_{0;1/2,\Gamma_N} := \|E_{N,0}(\xi)\|_{1/2,\partial\Omega} \qquad \forall\, \xi \in H_{00}^{1/2}(\Gamma_N)\,, \tag{2.3}$$

where $E_{N,0} : H^{1/2}(\Gamma_N) \to H^{1/2}(\partial\Omega)$ is the extension by zero in $\Gamma_D := \partial\Omega\backslash\bar{\Gamma}_N$. Alternatively, $H_{00}^{1/2}(\Gamma_N)$ is the interpolation space with index $1/2$ between $H_0^1(\Gamma_N)$ and $L^2(\Gamma_N)$ (cf. [38, Chapitre 1], [40, Appendix B]). In addition, from now on $\|\cdot\|_{0;-1/2,\Gamma_N}$ denotes the norm of $H_{00}^{-1/2}(\Gamma_N)$, and $\langle\cdot\,,\,\cdot\rangle_{\Gamma_N}$ stands for the corresponding duality pairing with respect to the $L^2(\Gamma_N)$ inner product.

Licensed to University of Oxford. Prepared on Fri Oct 16 07:02:22 EDT 2015 for download from IP 129.67.185.217.
License or copyright restrictions may apply to redistribution; see http://www.ams.org/journal-terms-of-use

## 3. The variational formulation

Multiplying by $\boldsymbol{v} \in \boldsymbol{H}(\mathrm{div};\Omega)$ the first equation of (2.2), integrating by parts, introducing the additional unknown $\lambda := -p|_{\Gamma_N} \in H^{1/2}_{00}(\Gamma_N)$, multiplying by $q \in L^2(\Omega)$ the second equation of (2.2), and imposing the Neumann condition in a weak fashion, we obtain the following saddle point problem: Find $(\boldsymbol{u},(p,\lambda)) \in \boldsymbol{H}\times\boldsymbol{Q}$ such that

$$\begin{array}{rcll} \boldsymbol{a}(\boldsymbol{u},\boldsymbol{v}) + \boldsymbol{b}(\boldsymbol{v},(p,\lambda)) & = & \gamma\displaystyle\int_\Omega p\,\boldsymbol{f}\cdot\boldsymbol{v} + \gamma\int_\Omega \boldsymbol{f}\cdot\boldsymbol{v} & \forall\,\boldsymbol{v}\in\boldsymbol{H}\,, \\ \boldsymbol{b}(\boldsymbol{u},(q,\xi)) & = & \langle g,\xi\rangle_{\Gamma_N} & \forall\,(q,\xi)\in\boldsymbol{Q}\,, \end{array} \tag{3.1}$$

where $\boldsymbol{H} := \boldsymbol{H}(\mathrm{div};\Omega)$, $\boldsymbol{Q} := L^2(\Omega)\times H^{1/2}_{00}(\Gamma_N)$, and $\boldsymbol{a} : \boldsymbol{H}\times\boldsymbol{H}\to\mathbb{R}$ and $\boldsymbol{b} : \boldsymbol{H}\times\boldsymbol{Q}\to\mathbb{R}$ are the bounded bilinear forms defined by

$$\begin{array}{ll} \boldsymbol{a}(\boldsymbol{u},\boldsymbol{v}) := \alpha_0\,\gamma\displaystyle\int_\Omega \boldsymbol{u}\cdot\boldsymbol{v} & \forall\,\boldsymbol{u},\,\boldsymbol{v}\in\boldsymbol{H}\,, \\ \boldsymbol{b}(\boldsymbol{v},(q,\xi)) := \displaystyle\int_\Omega q\,\mathrm{div}\,\boldsymbol{v} + \langle\boldsymbol{v}\cdot\boldsymbol{\nu},\xi\rangle_{\Gamma_N} & \forall\,(\boldsymbol{v},(q,\xi))\in\boldsymbol{H}\times\boldsymbol{Q}\,. \end{array} \tag{3.2}$$

The space $\boldsymbol{H}$ is provided with the usual norm of $\boldsymbol{H}(\mathrm{div};\Omega)$ (cf. (1.1)), whereas $\boldsymbol{Q}$ is endowed with the corresponding product norm, that is (cf. (2.3))

$$\|(q,\xi)\|_{\boldsymbol{Q}} := \|q\|_{0,\Omega} + \|\xi\|_{0;1/2,\Gamma_N} \qquad \forall\,(q,\xi)\in\boldsymbol{Q}\,. \tag{3.3}$$

Similarly, we set

$$\|(\boldsymbol{v},(q,\xi))\|_{\boldsymbol{H}\times\boldsymbol{Q}} := \|\boldsymbol{v}\|_{\boldsymbol{H}} + \|(q,\xi)\|_{\boldsymbol{Q}} \qquad \forall\,(\boldsymbol{v},(q,\xi))\in\boldsymbol{H}\times\boldsymbol{Q}\,. \tag{3.4}$$

Note now that actually (3.1) can be rewritten as: Find $(\boldsymbol{u},(p,\lambda))\in\boldsymbol{H}\times\boldsymbol{Q}$ such that

$$\begin{array}{rcll} \boldsymbol{a}(\boldsymbol{u},\boldsymbol{v}) + \boldsymbol{b}_1(\boldsymbol{v},(p,\lambda)) & = & \gamma\displaystyle\int_\Omega \boldsymbol{f}\cdot\boldsymbol{v} & \forall\,\boldsymbol{v}\in\boldsymbol{H}\,, \\ \boldsymbol{b}_2(\boldsymbol{u},(q,\xi)) & = & \langle g,\xi\rangle_{\Gamma_N} & \forall\,(q,\xi)\in\boldsymbol{Q}\,, \end{array} \tag{3.5}$$

where $\boldsymbol{b}_1 : \boldsymbol{H}\times\boldsymbol{Q}\to\mathbb{R}$ is the bounded bilinear form defined by

$$\boldsymbol{b}_1(\boldsymbol{v},(q,\xi)) := \int_\Omega q\,\mathrm{div}\,\boldsymbol{v} + \langle\boldsymbol{v}\cdot\boldsymbol{\nu},\xi\rangle_{\Gamma_N} - \gamma\int_\Omega q\,\boldsymbol{f}\cdot\boldsymbol{v} \qquad \forall\,(\boldsymbol{v},(q,\xi))\in\boldsymbol{H}\times\boldsymbol{Q}\,, \tag{3.6}$$

and $\boldsymbol{b}_2 = \boldsymbol{b}$ (cf. (3.2)), which constitutes a particular example of the generalized Babuška-Brezzi theory developed in [12]. Nevertheless, for ease of the analysis, in what follows we do not adopt this approach, but rather apply a combination of the classical Babuška-Brezzi theory and the Banach fixed point theorem.

We now assume additionally that $\boldsymbol{f}\in\boldsymbol{L}^\infty(\Omega)$. Then, it is clear that, given $r\in L^2(\Omega)$, the linear functionals $\boldsymbol{F}_r : \boldsymbol{H}\to\mathbb{R}$, $\boldsymbol{F} : \boldsymbol{H}\to\mathbb{R}$ and $\boldsymbol{G} : \boldsymbol{Q}\to\mathbb{R}$ defined by

$$\begin{array}{ll} \boldsymbol{F}_r(\boldsymbol{v}) := \gamma\displaystyle\int_\Omega r\,\boldsymbol{f}\cdot\boldsymbol{v} & \forall\,\boldsymbol{v}\in\boldsymbol{H}\,, \\ \boldsymbol{F}(\boldsymbol{v}) := \gamma\displaystyle\int_\Omega \boldsymbol{f}\cdot\boldsymbol{v} & \forall\,\boldsymbol{v}\in\boldsymbol{H}\,, \\ \boldsymbol{G}(q,\xi) := \langle g,\xi\rangle_{\Gamma_N} & \forall\,(q,\xi)\in\boldsymbol{Q}\,, \end{array} \tag{3.7}$$

Licensed to University of Oxford. Prepared on Fri Oct 16 07:02:22 EDT 2015 for download from IP 129.67.185.217.
License or copyright restrictions may apply to redistribution; see http://www.ams.org/journal-terms-of-use

satisfy

$$|\boldsymbol{F}_r(\boldsymbol{v})| \,\leq\, \gamma\,\|r\|_{0,\Omega}\,\|\boldsymbol{f}\|_{\infty,\Omega}\,\|\boldsymbol{v}\|_{0,\Omega} \quad \forall\,\boldsymbol{v}\in\boldsymbol{H}, \tag{3.8}$$

$$|\boldsymbol{F}(\boldsymbol{v})| \,\leq\, \gamma\,|\Omega|\,\|\boldsymbol{f}\|_{\infty,\Omega},\|\boldsymbol{v}\|_{0,\Omega} \quad \forall\,\boldsymbol{v}\in\boldsymbol{H}, \tag{3.9}$$

$$|\boldsymbol{G}(q,\,\xi)| \,\leq\, \|g\|_{0;-1/2,\Gamma_N}\,\|\xi\|_{0;1/2,\Gamma_N} \quad \forall\,(q,\xi)\in\boldsymbol{Q}\,, \tag{3.10}$$

which shows that $\boldsymbol{F}_r\in\boldsymbol{H}'$, $\boldsymbol{F}\in\boldsymbol{H}'$ and $\boldsymbol{G}\in\boldsymbol{Q}'$. Also, there clearly holds

$$|\boldsymbol{a}(\boldsymbol{u},\boldsymbol{v})| \,\leq\, \|\boldsymbol{a}\|\,\|\boldsymbol{u}\|_{\boldsymbol{H}}\,\|\boldsymbol{v}\|_{\boldsymbol{H}} \quad \forall\,\boldsymbol{u},\,\boldsymbol{v}\in\boldsymbol{H}$$

and

$$|\boldsymbol{b}(\boldsymbol{v},(q,\,\xi))| \,\leq\, \|\boldsymbol{b}\|\,\|\boldsymbol{v}\|_{\boldsymbol{H}}\,\|(q,\,\xi)\|_{\boldsymbol{Q}} \quad \forall\,(\boldsymbol{v},(q,\,\xi))\in\boldsymbol{H}\times\boldsymbol{Q}\,,$$

with $\|\boldsymbol{a}\| \,=\, \alpha_0\,\gamma$ and $\|\boldsymbol{b}\|$ depending on the normal trace operator in $\boldsymbol{H}(\mathrm{div};\Omega)$. In addition, the kernel of $\boldsymbol{b}$ can be readily characterized as:

$$\boldsymbol{V} \,:=\, \boldsymbol{N}(\boldsymbol{b}) \,=\, \Big\{\boldsymbol{v}\in\boldsymbol{H}(\mathrm{div};\Omega):\quad \mathrm{div}\,\boldsymbol{v}=0 \quad \text{in}\ \Omega\,,\quad \text{and}\quad \boldsymbol{v}\cdot\boldsymbol{\nu}=0\quad \text{on}\quad \Gamma_N\Big\}$$

and

$$\boldsymbol{a}(\boldsymbol{v},\boldsymbol{v}) \,=\, \alpha_0\,\gamma\,\|\boldsymbol{v}\|^2_{0,\Omega} \,=\, \alpha\,\|\boldsymbol{v}\|^2_{\boldsymbol{H}} \quad \forall\,\boldsymbol{v}\in\boldsymbol{V}\,,$$

with $\alpha \,:=\, \alpha_0\,\gamma$, and it is quite standard to see that there exists $\beta>0$ such that (cf. [27, Section 2.4.2])

$$\sup_{\substack{\boldsymbol{v}\in\boldsymbol{H}\\ \boldsymbol{v}\neq 0}}\frac{\boldsymbol{b}(\boldsymbol{v},(q,\xi))}{\|\boldsymbol{v}\|_{\boldsymbol{H}}} \,\geq\, \beta\,\|(q,\xi)\|_{\boldsymbol{Q}} \quad \forall\,(q,\xi)\in\boldsymbol{Q}\,.$$

In other words, $\boldsymbol{a}(\cdot,\cdot)$ is $\boldsymbol{V}$-elliptic and $\boldsymbol{b}(\cdot,\cdot)$ satisfies the continuous inf-sup condition on $\boldsymbol{H}\times\boldsymbol{Q}$, which, thanks to the Babuška-Brezzi theory, insures in advance that problems (3.15) and (3.17), which are introduced below, are well posed. In particular, this fact guarantees the continuous dependence result for the solution of each problem.

Consequently, we can introduce the affine operator $\boldsymbol{T}:\boldsymbol{H}\times\boldsymbol{Q}\to\boldsymbol{H}\times\boldsymbol{Q}$ that, given $(\boldsymbol{w},(r,\eta))\in\boldsymbol{H}\times\boldsymbol{Q}$, defines

$$\boldsymbol{T}(\boldsymbol{w},(r,\eta)) \,:=\, (\bar{\boldsymbol{u}},(\bar{p},\bar{\lambda}))\in\boldsymbol{H}\times\boldsymbol{Q} \tag{3.11}$$

as the unique solution of (3.1) when $p$ is replaced by $r$ on the right-hand side of $(3.1)_1$, that is,

$$\begin{array}{rcll} \boldsymbol{a}(\bar{\boldsymbol{u}},\boldsymbol{v})+\boldsymbol{b}(\boldsymbol{v},(\bar{p},\,\bar{\lambda})) &=& \boldsymbol{F}_r(\boldsymbol{v})+\boldsymbol{F}(\boldsymbol{v}) & \forall\,\boldsymbol{v}\in\boldsymbol{H}\,,\\ \boldsymbol{b}(\bar{\boldsymbol{u}},(q,\,\xi)) &=& \boldsymbol{G}(q,\,\xi) & \forall\,(q,\,\xi)\in\boldsymbol{Q}\,. \end{array} \tag{3.12}$$

In this way, our original problem (3.1) can be rewritten as: Find $(\boldsymbol{u},(p,\lambda))\in\boldsymbol{H}\times\boldsymbol{Q}$ such that

$$\boldsymbol{T}(\boldsymbol{u},(p,\lambda)) \,=\, (\boldsymbol{u},(p,\lambda)), \tag{3.13}$$

that is, to find a fixed point of $\boldsymbol{T}$, for which, as announced previously, we aim next to apply the Banach fixed point Theorem. To this end we first observe, from the superposition principle, that

$$\boldsymbol{T}(\boldsymbol{w},(r,\eta)) \,=\, (\boldsymbol{u}_0,(p_0,\lambda_0))+\boldsymbol{S}(\boldsymbol{w},(r,\eta)) \quad \forall\,(\boldsymbol{w},(r,\eta))\in\boldsymbol{H}\times\boldsymbol{Q}\,, \tag{3.14}$$

where $(\boldsymbol{u}_0,(p_0,\lambda_0))\in\boldsymbol{H}\times\boldsymbol{Q}$ is the unique solution of the auxiliary problem

$$\begin{array}{rcll} \boldsymbol{a}(\boldsymbol{u}_0,\boldsymbol{v})+\boldsymbol{b}(\boldsymbol{v},(p_0,\lambda_0)) &=& \boldsymbol{F}(\boldsymbol{v}) & \forall\,\boldsymbol{v}\in\boldsymbol{H}\,,\\ \boldsymbol{b}(\boldsymbol{u}_0,(q,\xi)) &=& \boldsymbol{G}(q,\xi) & \forall\,(q,\xi)\in\boldsymbol{Q}\,, \end{array} \tag{3.15}$$

Licensed to University of Oxford. Prepared on Fri Oct 16 07:02:22 EDT 2015 for download from IP 129.67.185.217.
License or copyright restrictions may apply to redistribution; see http://www.ams.org/journal-terms-of-use

and $\boldsymbol{S} : \boldsymbol{H} \times \boldsymbol{Q} \to \boldsymbol{H} \times \boldsymbol{Q}$ is the linear operator that, given $(\boldsymbol{w}, (r, \eta)) \in \boldsymbol{H} \times \boldsymbol{Q}$, defines

$$\boldsymbol{S}(\boldsymbol{w}, (r, \eta)) := (\widehat{\boldsymbol{u}}, (\widehat{p}, \widehat{\lambda})) \in \boldsymbol{H} \times \boldsymbol{Q} \tag{3.16}$$

as the unique solution of (3.12) with $\boldsymbol{F}$ and $\boldsymbol{G}$ replaced by null functionals, that is,

$$\begin{array}{rcll} \boldsymbol{a}(\widehat{\boldsymbol{u}}, \boldsymbol{v}) + \boldsymbol{b}(\boldsymbol{v}, (\widehat{p}, \widehat{\lambda})) & = & \boldsymbol{F}_r(\boldsymbol{v}) & \forall\, \boldsymbol{v} \in \boldsymbol{H}\,, \\ \boldsymbol{b}(\widehat{\boldsymbol{u}}, (q, \xi)) & = & 0 & \forall\, (q, \xi) \in \boldsymbol{Q}\,. \end{array} \tag{3.17}$$

Note here that (3.14) confirms the term affine given in advance to $\boldsymbol{T}$.

Furthermore, the continuous dependence result for (3.15) and (3.17) establishes the existence of a same constant $\tilde{C} := \tilde{C}(\|\boldsymbol{a}\|, \alpha, \beta) > 0$ such that

$$\|(\boldsymbol{u}_0, (p_0, \lambda_0))\|_{\boldsymbol{H}\times\boldsymbol{Q}} \leq \tilde{C} \left\{ \|\boldsymbol{F}\|_{\boldsymbol{H}'} + \|\boldsymbol{G}\|_{\boldsymbol{Q}'} \right\} \tag{3.18}$$

and

$$\|\boldsymbol{S}(\boldsymbol{w}, (r, \eta))\|_{\boldsymbol{H}\times\boldsymbol{Q}} \leq \tilde{C} \|\boldsymbol{F}_r\|_{\boldsymbol{H}'}\,. \tag{3.19}$$

In particular, (3.19) and (3.8) yield

$$\|\boldsymbol{S}(\boldsymbol{w}, (r, \eta))\|_{\boldsymbol{H}\times\boldsymbol{Q}} \leq \tilde{C}\, \gamma\, \|\boldsymbol{f}\|_{\infty,\Omega}\, \|r\|_{0,\Omega} \quad \forall\, (\boldsymbol{w}, (r, \eta)) \in \boldsymbol{H} \times \boldsymbol{Q}\,,$$

and hence, given $(\boldsymbol{w}_1, (r_1, \eta_1))$, $(\boldsymbol{w}_2, (r_2, \eta_2)) \in \boldsymbol{H} \times \boldsymbol{Q}$, we can use (3.14) to find that

$$\begin{aligned} &\|\boldsymbol{T}(\boldsymbol{w}_1, (r_1, \eta_1)) - \boldsymbol{T}(\boldsymbol{w}_2, (r_2, \eta_2))\|_{\boldsymbol{H}\times\boldsymbol{Q}} \\ &\quad = \|\boldsymbol{S}\big((\boldsymbol{w}_1, (r_1, \eta_1)) - (\boldsymbol{w}_2, (r_2, \eta_2))\big)\|_{\boldsymbol{H}\times\boldsymbol{Q}} \\ &\quad \leq \tilde{C}\, \gamma\, \|\boldsymbol{f}\|_{\infty,\Omega}\, \|r_1 - r_2\|_{0,\Omega} \\ &\quad \leq \tilde{C}\, \gamma\, \|\boldsymbol{f}\|_{\infty,\Omega}\, \|(\boldsymbol{w}_1, (r_1, \eta_1)) - (\boldsymbol{w}_2, (r_2, \eta_2))\|_{\boldsymbol{H}\times\boldsymbol{Q}}\,, \end{aligned}$$

which shows that $\boldsymbol{T}$ is a contraction if $\|\boldsymbol{f}\|_{\infty,\Omega} < \frac{1}{\tilde{C}\,\gamma}$. We have thus proved the following result.

**Theorem 3.1.** *Assume that $\boldsymbol{f} \in \boldsymbol{L}^\infty(\Omega)$ and that $\|\boldsymbol{f}\|_{\infty,\Omega} < \frac{1}{\tilde{C}\,\gamma}$. Then, there exists a unique $(\boldsymbol{u}, (p, \lambda)) \in \boldsymbol{H} \times \boldsymbol{Q}$ solution of our variational formulation* (3.1). *Moreover, there holds*

$$\begin{aligned} \|\boldsymbol{u}\|_{\boldsymbol{H}} + \big\{1 - \tilde{C}\,\gamma\, \|\boldsymbol{f}\|_{\infty,\Omega}\big\}\, \|(p, \lambda)\|_{\boldsymbol{Q}} &\leq \tilde{C} \left\{ \|\boldsymbol{F}\|_{\boldsymbol{H}'} + \|\boldsymbol{G}\|_{\boldsymbol{Q}'} \right\} \\ &\leq \tilde{C} \left\{ \gamma\, |\Omega|\, \|\boldsymbol{f}\|_{\infty,\Omega} + \|g\|_{0;-1/2,\Gamma_N} \right\}. \end{aligned} \tag{3.20}$$

*Proof.* According to the foregoing analysis, the unique solvability of (3.1) follows straightforwardly from the Banach fixed point Theorem, and hence it only remains to show (3.20). For this purpose, we first observe, using (3.13) and (3.14), that

$$\|\boldsymbol{u}\|_{\boldsymbol{H}} + \|(p, \lambda)\|_{\boldsymbol{Q}} = \|\boldsymbol{T}(\boldsymbol{u}, (p, \lambda))\|_{\boldsymbol{H}\times\boldsymbol{Q}} = \|(\boldsymbol{u}_0, (p_0, \lambda_0)) + \boldsymbol{S}(\boldsymbol{u}, (p, \lambda))\|_{\boldsymbol{H}\times\boldsymbol{Q}}\,,$$

which, thanks to the triangle inequality and the estimates (3.18) and (3.19), leads to

$$\|\boldsymbol{u}\|_{\boldsymbol{H}} + \|(p, \lambda)\|_{\boldsymbol{Q}} \leq \tilde{C} \left\{ \|\boldsymbol{F}\|_{\boldsymbol{H}'} + \|\boldsymbol{G}\|_{\boldsymbol{Q}'} + \|\boldsymbol{F}_p\|_{\boldsymbol{H}'} \right\}. \tag{3.21}$$

In turn, it is clear from (3.8), (3.9), and (3.10), that

$$\|\boldsymbol{F}_p\|_{\boldsymbol{H}'} \leq \gamma\, \|\boldsymbol{f}\|_{\infty,\Omega}\, \|(p, \lambda)\|_{\boldsymbol{Q}}\,, \quad \|\boldsymbol{F}\|_{\boldsymbol{H}'} \leq \gamma\, |\Omega|\, \|\boldsymbol{f}\|_{\infty,\Omega}$$

Licensed to University of Oxford. Prepared on Fri Oct 16 07:02:22 EDT 2015 for download from IP 129.67.185.217.
License or copyright restrictions may apply to redistribution; see http://www.ams.org/journal-terms-of-use

and

$$\|\boldsymbol{G}\|_{\boldsymbol{Q}'} \,\leq\, \|g\|_{0;-1/2,\Gamma_N},$$

which, together with (3.21), yield the inequalities in (3.20) and complete the proof. □

In particular, if we assume in Theorem 3.1 that $\|\boldsymbol{f}\|_{\infty,\Omega} \,\leq\, \frac{1}{2\,\tilde{C}\,\gamma}$, we deduce that

$$2\,\|\boldsymbol{u}\|_{\boldsymbol{H}} \,+\, \|(p,\lambda)\|_{\boldsymbol{Q}} \,\leq\, 2\,\tilde{C}\,\Big\{\|\boldsymbol{F}\|_{\boldsymbol{H}'} \,+\, \|\boldsymbol{G}\|_{\boldsymbol{Q}'}\Big\}. \tag{3.22}$$

The converse of the derivation of (3.1) is provided now. More precisely, the following theorem establishes that the unique solution of (3.1) solves the original boundary value problem (2.2). This result is employed later on in Section 5.3 to show the efficiency of the a posteriori error estimator derived previously in Section 5.2.

**Theorem 3.2.** *Let* $(\boldsymbol{u},(p,\lambda)) \in \boldsymbol{H}\times\boldsymbol{Q}$ *be the unique solution of* (3.1). *Then* $\operatorname{div}\boldsymbol{u}=0$ *in* $\Omega$, $\boldsymbol{u}\cdot\boldsymbol{\nu}=g$ *on* $\Gamma_N$, $\nabla p=-(\gamma\,\boldsymbol{f}+\gamma\,p\,\boldsymbol{f}-\alpha_0\,\gamma\,\boldsymbol{u})$ *in* $\Omega$ (*which yields* $p\in H^1(\Omega)$), $p=0$ *on* $\Gamma_D$, *and* $\lambda=-p$ *on* $\Gamma_N$.

*Proof.* It follows by applying integration by parts backwards in (3.1) and then using suitable test functions. We omit further details. □

## 4. The Galerkin scheme

4.1. **Main results.** Let $\boldsymbol{H}_h$ and $\boldsymbol{Q}_h$ be finite dimensional subspaces of $\boldsymbol{H}$ and $\boldsymbol{Q}$, respectively, and consider the Galerkin scheme: Find $(\boldsymbol{u}_h,(p_h,\lambda_h)) \in \boldsymbol{H}_h\times\boldsymbol{Q}_h$ such that

$$\begin{aligned} \boldsymbol{a}(\boldsymbol{u}_h,\boldsymbol{v}_h) \,+\, \boldsymbol{b}(\boldsymbol{v}_h,(p_h,\lambda_h)) &= \gamma\int_\Omega p_h\,\boldsymbol{f}\cdot\boldsymbol{v}_h \,+\, \gamma\int_\Omega \boldsymbol{f}\cdot\boldsymbol{v}_h \quad \forall\,\boldsymbol{v}_h\in\boldsymbol{H}_h\,, \\ \boldsymbol{b}(\boldsymbol{u}_h,(q_h,\xi_h)) &= \langle g,\xi_h\rangle_{\Gamma_N} \quad \forall\,(q_h,\xi_h)\in\boldsymbol{Q}_h. \end{aligned} \tag{4.1}$$

Then, we let $\boldsymbol{V}_h$ be the discrete kernel of $\boldsymbol{b}$, that is,

$$\boldsymbol{V}_h \,:=\, \Big\{\boldsymbol{v}_h\in\boldsymbol{H}_h:\quad \boldsymbol{b}(\boldsymbol{v}_h,(q_h,\xi_h))=0 \quad \forall\,(q_h,\xi_h)\in\boldsymbol{Q}_h\Big\}, \tag{4.2}$$

and assume that there exists $\widehat{\alpha}>0$, independent of $h$, such that

$$\boldsymbol{a}(\boldsymbol{v}_h,\boldsymbol{v}_h) \,\geq\, \widehat{\alpha}\,\|\boldsymbol{v}_h\|^2_{\boldsymbol{H}} \quad \forall\,\boldsymbol{v}_h\in\boldsymbol{V}_h\,. \tag{4.3}$$

In addition, we also suppose that there exists $\widehat{\beta}>0$, independent of $h$, such that

$$\sup_{\substack{\boldsymbol{v}_h\in\boldsymbol{H}_h\\ \boldsymbol{v}_h\neq 0}} \frac{\boldsymbol{b}(\boldsymbol{v}_h,(q_h,\xi_h))}{\|\boldsymbol{v}_h\|_{\boldsymbol{H}_h}} \,\geq\, \widehat{\beta}\,\|(q_h,\xi_h)\|_{\boldsymbol{Q}_h} \quad \forall\,(q_h,\xi_h)\in\boldsymbol{Q}_h\,. \tag{4.4}$$

Specific finite element subspaces $\boldsymbol{H}_h$ and $\boldsymbol{Q}_h$ satisfying (4.3) and (4.4) will be indicated below in Section 4.2. Then, introducing corresponding discrete operators $\boldsymbol{T}_h:\boldsymbol{H}_h\times\boldsymbol{Q}_h\to\boldsymbol{H}_h\times\boldsymbol{Q}_h$ and $\boldsymbol{S}_h:\boldsymbol{H}_h\times\boldsymbol{Q}_h\to\boldsymbol{H}_h\times\boldsymbol{Q}_h$, and the particular discrete solutions $(\boldsymbol{u}_{h,0},(p_{h,0},\lambda_{h,0}))\in\boldsymbol{H}_h\times\boldsymbol{Q}_h$, analogously to the definitions given for the continuous case (cf. (3.11), (3.14), (3.16)), we find that (4.1) is equivalent to the fixed point equation: Find $(\boldsymbol{u}_h,(p_h,\lambda_h))\in\boldsymbol{H}_h\times\boldsymbol{Q}_h$ such that

$$\boldsymbol{T}_h(\boldsymbol{u}_h,(p_h,\lambda_h)) \,=\, (\boldsymbol{u}_h,(p_h,\lambda_h)),$$

Licensed to University of Oxford. Prepared on Fri Oct 16 07:02:22 EDT 2015 for download from IP 129.67.185.217.
License or copyright restrictions may apply to redistribution; see http://www.ams.org/journal-terms-of-use

where

$$\boldsymbol{T}_h(\boldsymbol{w}_h,(r_h,\eta_h)) \,=\, (\boldsymbol{u}_{h,0},(p_{h,0},\lambda_{h,0})) \,+\, \boldsymbol{S}_h(\boldsymbol{w}_h,(r_h,\eta_h)) \qquad \forall\,(\boldsymbol{w}_h,(r_h,\eta_h)) \in \boldsymbol{H}_h\times\boldsymbol{Q}_h\,.$$

Hence, using the same arguments from the proof of Theorem 3.1, we deduce the following result.

**Theorem 4.1.** *Assume that* $\boldsymbol{f}\in\boldsymbol{L}^\infty(\Omega)$ *and that* $\|\boldsymbol{f}\|_{\infty,\Omega}\,\leq\,\frac{1}{2\,\widehat{C}\,\gamma}$, *where* $\widehat{C}\,:=\,\widehat{C}(\|\boldsymbol{a}\|,\widehat{\alpha},\widehat{\beta})$ *is the continuous dependence constant for the discrete problems defining* $(\boldsymbol{u}_{h,0},(p_{h,0},\lambda_{h,0}))$ *and the operator* $\boldsymbol{S}_h$. *Then, there exists a unique* $(\boldsymbol{u}_h,(p_h,\lambda_h))$ *solution of* (4.1), *and there holds*

$$2\,\|\boldsymbol{u}_h\|_{\boldsymbol{H}}\,+\,\|(p_h,\lambda_h)\|_{\boldsymbol{Q}}\,\leq\,2\,\widehat{C}\left\{\gamma\,|\Omega|\,\|\boldsymbol{f}\|_{\infty,\Omega}\,+\,\|g\|_{0;-1/2,\Gamma_N}\right\}.$$

On the other hand, in order to derive the Cea estimate for (4.1), we now take arbitrary functionals $\mathcal{F}\in\boldsymbol{H}'$, $\mathcal{G}\in\boldsymbol{Q}'$, $\mathcal{F}_h\in\boldsymbol{H}_h'$, and $\mathcal{G}_h\in\boldsymbol{Q}_h'$, and consider the following continuous and discrete problems:

**(P)** Find $(\boldsymbol{w},(r,\eta))\in\boldsymbol{H}\times\boldsymbol{Q}$ such that

$$\begin{aligned}\boldsymbol{a}(\boldsymbol{w},\boldsymbol{v})+\boldsymbol{b}(\boldsymbol{v},(r,\eta)) &= \mathcal{F}(\boldsymbol{v}) \qquad \forall\,\boldsymbol{v}\in\boldsymbol{H}\,,\\ \boldsymbol{b}(\boldsymbol{w},(q,\xi)) &= \mathcal{G}(q,\xi) \qquad \forall\,(q,\xi)\in\boldsymbol{Q}\,.\end{aligned}$$

**($\mathbf{P}_h$)** Find $(\boldsymbol{w}_h,(r_h,\eta_h))\in\boldsymbol{H}_h\times\boldsymbol{Q}_h$ such that

$$\begin{aligned}\boldsymbol{a}(\boldsymbol{w}_h,\boldsymbol{v}_h)+\boldsymbol{b}(\boldsymbol{v}_h,(r_h,\eta_h)) &= \mathcal{F}_h(\boldsymbol{v}_h) \qquad \forall\,\boldsymbol{v}_h\in\boldsymbol{H}_h\,,\\ \boldsymbol{b}(\boldsymbol{w}_h,(q_h,\xi_h)) &= \mathcal{G}_h(q_h,\xi_h) \qquad \forall\,(q_h,\xi_h)\in\boldsymbol{Q}_h\,.\end{aligned}$$

The corresponding Strang-type error estimate for **(P)** and **($\mathbf{P}_h$)** establishes in this case (cf. [49]) that

$$\begin{aligned}\|\boldsymbol{w}-\boldsymbol{w}_h\|_{\boldsymbol{H}} \leq\, &\left(1+\frac{\|\boldsymbol{a}\|}{\widehat{\alpha}}\right)\left(1+\frac{\|\boldsymbol{b}\|}{\widehat{\beta}}\right)\,\mathrm{dist}(\boldsymbol{w},\boldsymbol{H}_h)\,+\,\frac{\|\boldsymbol{b}\|}{\widehat{\alpha}}\,\mathrm{dist}((r,\eta),\boldsymbol{Q}_h)\\ &+\,\frac{1}{\widehat{\beta}}\left(1+\frac{\|\boldsymbol{a}\|}{\widehat{\alpha}}\right)\,\|\mathcal{G}_h-\mathcal{G}\|_{\boldsymbol{Q}_h'}\,+\,\frac{1}{\widehat{\alpha}}\,\|\mathcal{F}_h-\mathcal{F}\|_{\boldsymbol{H}_h'}\,,\end{aligned}\tag{4.5}$$

(4.6)

$$\begin{aligned}\|(r,\eta)-(r_h,\eta_h)\|_{\boldsymbol{Q}} \leq\, &\frac{\|\boldsymbol{a}\|}{\widehat{\beta}}\,\left(1+\frac{\|\boldsymbol{a}\|}{\widehat{\alpha}}\right)\left(1+\frac{\|\boldsymbol{b}\|}{\widehat{\beta}}\right)\,\mathrm{dist}(\boldsymbol{w},\boldsymbol{H}_h)\\ &+\left(1+\frac{\|\boldsymbol{b}\|}{\widehat{\beta}}\,+\,\frac{\|\boldsymbol{a}\|\,\|\boldsymbol{b}\|}{\widehat{\alpha}\,\widehat{\beta}}\right)\,\mathrm{dist}((r,\eta),Q_h)\\ &+\frac{\|\boldsymbol{a}\|}{\widehat{\beta}^2}\,\left(1+\frac{\|\boldsymbol{a}\|}{\widehat{\alpha}}\right)\,\|\mathcal{G}_h-\mathcal{G}\|_{\boldsymbol{Q}_h'}+\frac{1}{\widehat{\beta}}\,\left(1+\frac{\|\boldsymbol{a}\|}{\widehat{\alpha}}\right)\,\|\mathcal{F}_h-\mathcal{F}\|_{\boldsymbol{H}_h'}\,.\end{aligned}$$

Hence, applying (4.5) and (4.6) to the continuous and discrete schemes given by (3.1) and (4.1), which means taking

$$\begin{aligned}\mathcal{F}(\boldsymbol{v}) &:= \gamma\int_\Omega p\,\boldsymbol{f}\cdot\boldsymbol{v}\,+\,\gamma\int_\Omega\boldsymbol{f}\cdot\boldsymbol{v}\,=\,\boldsymbol{F}_p(\boldsymbol{v})\,+\,\boldsymbol{F}(\boldsymbol{v}) \qquad \forall\,\boldsymbol{v}\in\boldsymbol{H},\\ \mathcal{F}_h(\boldsymbol{v}_h) &:= \gamma\int_\Omega p_h\,\boldsymbol{f}\cdot\boldsymbol{v}_h\,+\,\gamma\int_\Omega\boldsymbol{f}\cdot\boldsymbol{v}_h\,=\,\boldsymbol{F}_{p_h}(\boldsymbol{v}_h)\,+\,\boldsymbol{F}(\boldsymbol{v}_h) \qquad \forall\,\boldsymbol{v}_h\in\boldsymbol{H}_h,\end{aligned}$$

Licensed to University of Oxford. Prepared on Fri Oct 16 07:02:22 EDT 2015 for download from IP 129.67.185.217.
License or copyright restrictions may apply to redistribution; see http://www.ams.org/journal-terms-of-use

$\mathcal{G} := \boldsymbol{G}$, and $\mathcal{G}_h := \boldsymbol{G}|_{\boldsymbol{Q}_h}$, we deduce, with the constants $\widehat{C}_1$, $\widehat{C}_2$, $\widehat{C}_3$, and $\widehat{C}_4$ suggested by (4.5) and (4.6), that

$$\|\boldsymbol{u}-\boldsymbol{u}_h\|_{\boldsymbol{H}} \,\leq\, \widehat{C}_1\,\mathrm{dist}(\boldsymbol{u},\boldsymbol{H}_h) \,+\, \widehat{C}_2\,\mathrm{dist}((p,\lambda),\boldsymbol{Q}_h) \,+\, \frac{1}{\widehat{\alpha}}\,\|\boldsymbol{F}_{p-p_h}\|_{\boldsymbol{H}_h'}$$

and

$$\begin{aligned}\|(p,\lambda)-(p_h,\lambda_h)\|_{\boldsymbol{Q}} \leq \widehat{C}_3\,\mathrm{dist}(\boldsymbol{u},\boldsymbol{H}_h) + \widehat{C}_4\,\mathrm{dist}((p,\lambda),\boldsymbol{Q}_h)\\ + \frac{1}{\widehat{\beta}}\left(1+\frac{\|\boldsymbol{a}\|}{\widehat{\alpha}}\right)\|\boldsymbol{F}_{p-p_h}\|_{\boldsymbol{H}_h'}\,,\end{aligned} \tag{4.7}$$

where, according to (3.8),

$$\|\boldsymbol{F}_{p-p_h}\|_{\boldsymbol{H}_h'} \,\leq\, \gamma\,\|\boldsymbol{f}\|_{\infty,\Omega}\,\|(p,\lambda)-(p_h,\lambda_h)\|_{\boldsymbol{Q}}\,. \tag{4.8}$$

Then, replacing (4.8) into (4.7), and assuming that

$$\frac{\gamma}{\widehat{\beta}}\left(1+\frac{\|\boldsymbol{a}\|}{\widehat{\alpha}}\right)\|\boldsymbol{f}\|_{\infty,\Omega} \,=\, \frac{\gamma\,(\widehat{\alpha}+\|\boldsymbol{a}\|)}{\widehat{\alpha}\,\widehat{\beta}}\,\|\boldsymbol{f}\|_{\infty,\Omega} \,<\, 1\,,$$

we can write, in particular,

$$\|\boldsymbol{f}\|_{\infty,\Omega} \,\leq\, \frac{\widehat{\alpha}\,\widehat{\beta}}{2\,\gamma\,(\widehat{\alpha}+\|\boldsymbol{a}\|)}\,,$$

and therefore we can assert that

$$\|(p,\lambda)-(p_h,\lambda_h)\|_{\boldsymbol{Q}} \,\leq\, 2\,\widehat{C}_3\,\mathrm{dist}(\boldsymbol{u},\boldsymbol{H}_h) \,+\, 2\,\widehat{C}_4\,\mathrm{dist}((p,\lambda),\boldsymbol{Q}_h)$$

and

$$\|\boldsymbol{u}-\boldsymbol{u}_h\|_{\boldsymbol{H}} \leq \widehat{C}_1\,\mathrm{dist}(\boldsymbol{u},\boldsymbol{H}_h) + \widehat{C}_2\,\mathrm{dist}((p,\lambda),\boldsymbol{Q}_h) + \frac{\gamma}{\widehat{\alpha}}\,\|\boldsymbol{f}\|_{\infty,\Omega}\,\|(p,\lambda)-(p_h,\lambda_h)\|_{\boldsymbol{Q}}\,.$$

Summarizing, and bearing in mind Theorems 3.1 and 4.1, we can state the following main result.

**Theorem 4.2.** *Assume that* $\boldsymbol{f}\in\boldsymbol{L}^\infty(\Omega)$ *and that*

$$\|\boldsymbol{f}\|_{\infty,\Omega} \,\leq\, \frac{1}{2\,\gamma}\,\min\left\{\frac{1}{\tilde{C}},\frac{1}{\widehat{C}},\frac{\widehat{\alpha}\,\widehat{\beta}}{\widehat{\alpha}+\|\boldsymbol{a}\|}\right\}\,,$$

*where* $\tilde{C}=\tilde{C}(\|\boldsymbol{a}\|,\alpha,\beta)>0$ *and* $\widehat{C}=\widehat{C}(\|\boldsymbol{a}\|,\widehat{\alpha},\widehat{\beta})>0$ *are the continuous dependence constants specified above. Then, the continuous and discrete problems* (3.1) *and* (4.1) *have unique solutions* $(\boldsymbol{u},(p,\lambda))\in\boldsymbol{H}\times\boldsymbol{Q}$ *and* $(\boldsymbol{u}_h,(p_h,\lambda_h))\in\boldsymbol{H}_h\times\boldsymbol{Q}_h$. *Moreover, there exists a constant* $C>0$, *depending on* $\|\boldsymbol{a}\|$, $\|\boldsymbol{b}\|$, $\widehat{\alpha}$, $\widehat{\beta}$, $\gamma$, *and* $\|\boldsymbol{f}\|_{\infty,\Omega}$, *such that*

$$\|(\boldsymbol{u},(p,\lambda))-(\boldsymbol{u}_h,(p_h,\lambda_h))\|_{\boldsymbol{H}\times\boldsymbol{Q}} \,\leq\, C\,\mathrm{dist}\Big((\boldsymbol{u},(p,\lambda)),\boldsymbol{H}_h\times\boldsymbol{Q}_h\Big)\,.$$

4.2. **Specific finite element subspaces.** We now assume that $\Omega$ is a polyhedral region of $\mathbb{R}^d$ and proceed to define explicit finite element subspaces of $\boldsymbol{H} := \boldsymbol{H}(\mathrm{div};\Omega)$ and $\boldsymbol{Q} := L^2(\Omega)\times H^{1/2}_{00}(\Gamma_N)$ satisfying the $\boldsymbol{V}_h$-ellipticity (4.3) and the discrete inf-sup condition (4.4). For this purpose, we let $\{\mathcal{T}_h\}_{h>0}$ be a shape-regular family of discretizations of $\bar{\Omega}$ into triangles $T$ (in $\mathbb{R}^2$) or tetrahedra $T$ (in $\mathbb{R}^3$) of diameter $h_T$, with meshsize $h:=\max\Big\{h_T:\quad T\in\mathcal{T}_h\Big\}$, and such that the partitions of $\Gamma_N$ and $\Gamma_D$ inherited from $\mathcal{T}_h$ coincide on $\bar{\Gamma}_D\cap\bar{\Gamma}_N$. We recall here, denoting by

Licensed to University of Oxford. Prepared on Fri Oct 16 07:02:22 EDT 2015 for download from IP 129.67.185.217.
License or copyright restrictions may apply to redistribution; see http://www.ams.org/journal-terms-of-use

$\rho_T$ the diameter of the largest ball contained in $T$, that shape-regularity of $\{\mathcal{T}_h\}_{h>0}$ means that there exists a constant $\sigma > 0$ such that

$$\frac{h_T}{\rho_T} \leq \sigma \ \forall\, T \in \mathcal{T}_h, \ \forall\, h > 0.$$

Also, given an integer $k \geq 0$ and a subset $S$ of $\mathbb{R}^d$, we denote by $P_k(S)$ the space of polynomials defined in $S$ of total degree at most $k$. Then, for each integer $k \geq 0$ and for each $T \in \mathcal{T}_h$, we recall the definition of the local Raviart-Thomas space of order $k$ as (see, e.g. [15], [49]) $\mathbf{RT}_k(T) := \mathbf{P}_k(T) \oplus P_k(T)\,\boldsymbol{x}$, where

$$\boldsymbol{x} := \begin{pmatrix} x_1 \\ \vdots \\ x_d \end{pmatrix}$$

is a generic vector of $\mathbb{R}^d$, $P_k(T)\,\boldsymbol{x} := \big\{\mathbf{q} : T \to \mathbb{R}^d : \ \mathbf{q}(\boldsymbol{x}) := p(\boldsymbol{x})\,\boldsymbol{x} \ \forall\, \boldsymbol{x} \in T\,, \ \text{for some } p \in P_k(T)\big\}$ and, according to the notation introduced in Section 1, $\mathbf{P}_k(T) := [P_k(T)]^d$.

Then, given an integer $k \geq 0$, we define the finite element subspace $\boldsymbol{H}_h$ for the approximation of $\boldsymbol{u} \in \boldsymbol{H}(\mathrm{div};\Omega)$ as the global Raviart-Thomas space of order $k$, that is,

$$\boldsymbol{H}_h := \Big\{\boldsymbol{v}_h \in \boldsymbol{H}(\mathrm{div};\Omega) : \quad \boldsymbol{v}_h|_T \in \mathbf{RT}_k(T) \quad \forall\, T \in \mathcal{T}_h\Big\}. \tag{4.9}$$

In turn, the finite element subspace for the pressure $p$ is given by the global space of piecewise polynomials of degree $\leq k$, that is,

$$Q_h^p := \Big\{q_h \in L^2(\Omega) : \quad q_h|_T \in P_k(T) \quad \forall\, T \in \mathcal{T}_h\Big\}. \tag{4.10}$$

Next, in order to define the finite element subspace for $\lambda$, we first let $\Gamma_{N,h}$ be the partition of $\Gamma_N$ inherited from the triangulation $\mathcal{T}_h$, and define the meshsize $h_N := \max\big\{|e| : \quad e \in \Gamma_{N,h}\big\}$. Note here that $e$ denotes either edges of triangles (in $\mathbb{R}^2$) or faces of tetrahedra (in $\mathbb{R}^3$). Then, we let $\Gamma_{N,\tilde{h}}$ be another partition of $\Gamma_N$, independent of $\Gamma_{N,h}$, and define $\tilde{h}_N := \max\Big\{|e| : \quad e \in \Gamma_{N,\tilde{h}}\Big\}$. Then, for the same integer $k \geq 0$ employed in the definitions (4.9) and (4.10), we introduce

$$Q_{\tilde{h}}^{\lambda} := \Big\{\xi_{\tilde{h}} \in H_{00}^{1/2}(\Gamma_N) : \quad \xi_{\tilde{h}}|_e \in P_{k+1}(e) \quad \forall\, e \in \Gamma_{N,\tilde{h}}\Big\}, \tag{4.11}$$

and then set

$$\boldsymbol{Q}_{h,\tilde{h}} := Q_h^p \times Q_{\tilde{h}}^{\lambda}. \tag{4.12}$$

According to the above definitions of $\boldsymbol{H}_h$ and $Q_h^p$, it is clear that $\mathrm{div}\,\boldsymbol{H}_h \subseteq Q_h^p$, which implies that the discrete kernel of $\boldsymbol{b}$ (cf. (4.2)) becomes

$$\boldsymbol{V}_h := \Big\{\boldsymbol{v}_h \in \boldsymbol{H}_h : \quad \mathrm{div}\,\boldsymbol{v}_h = 0 \quad \text{in} \quad \Omega\,, \quad \text{and} \quad \langle \boldsymbol{v}_h \cdot \boldsymbol{\nu}, \xi_{\tilde{h}} \rangle_{\Gamma_N} = 0 \quad \forall\, \xi_{\tilde{h}} \in Q_{\tilde{h}}^{\lambda}\Big\},$$

and hence the $\boldsymbol{V}_h$-ellipticity of $\boldsymbol{a}$ (cf. (4.3)) follows straightforwardly from the free divergence property satisfied by this subspace. Though it is not required by any subsequent analysis, we notice that the second condition defining $\boldsymbol{V}_h$ does not necessarily imply that $\boldsymbol{v}_h \cdot \boldsymbol{\nu}$ vanishes on $\Gamma_N$ for each $\boldsymbol{v}_h \in \boldsymbol{V}_h$.

Now, concerning the discrete inf-sup condition for $\boldsymbol{b}$ (cf. (4.4)), we omit detailed explanations and just observe that it actually follows from a slight modification of the analysis provided in [9, Lemmas 3.1, 3.2, and 3.3] for the case $k = 0$ in $\mathbb{R}^2$. More

Licensed to University of Oxford. Prepared on Fri Oct 16 07:02:22 EDT 2015 for download from IP 129.67.185.217.
License or copyright restrictions may apply to redistribution; see http://www.ams.org/journal-terms-of-use

precisely, assuming additionally that $\{\mathcal{T}_h\}_{h>0}$ is quasi-uniform in a neighborhood of $\Gamma_N$, the arguments from [9] can be easily extended to $\mathbb{R}^d$ ($d \in \{2,3\}$) and for any integer $k \geq 1$, thus showing the existence of constants $C_0 \in ]0,1]$ and $\widehat{\beta} > 0$, both independent of $h$ and $\tilde{h}$, such that (4.4) holds whenever $h_N \leq C_0\, \tilde{h}_N$. Certainly, this restriction on the meshsizes should be incorporated in the statements of Theorems 4.1 and 4.2 when the subspaces $\boldsymbol{H}_h$ and $\boldsymbol{Q}_{h,\tilde{h}}$ given by (4.9) and (4.12) are employed.

In addition to the foregoing discussion, it is important to remark that a simplification in the definition of the finite element subspace for $\lambda$ is possible in the two-dimensional case when $k = 0$. In fact, let us first assume, without loss of generality, that the number of edges of $\Gamma_{N,h}$ is an even number. The case of an odd number of edges is easily reduced to the even one by replacing any particular pair of adjacent edges by a single edge. Then, we let $\Gamma_{N,2h}$ be the partition of $\Gamma_N$ arising by joining pairs of adjacent elements of $\Gamma_{N,h}$, and define

$$Q_h^\lambda := \left\{ \xi_h \in H_{00}^{1/2}(\Gamma_N) : \quad \xi_h|_e \in P_1(e) \quad \forall\, e \in \Gamma_{N,2h} \right\}, \tag{4.13}$$

so that instead of $\boldsymbol{Q}_{h,\tilde{h}}$ we now set

$$\boldsymbol{Q}_h := Q_h^p \times Q_h^\lambda .$$

In this case, the discrete inf-sup condition for $\boldsymbol{b}$ (cf. (4.4)) does not need any quasi-uniformity assumption around $\Gamma_N$ nor any restriction on the meshsizes, and it basically follows by applying [32, Lemma 4.2], the analysis from [32, Section 5.1], and the recent result provided by [39, Theorem 5.1].

We end this description of specific finite element subspaces by mentioning that, for practical purposes, particularly for the implementation of the examples reported below in Section 6, the restriction on the meshsizes required by the discrete inf-sup condition (4.4) (for $k \geq 1$ in $\mathbb{R}^2$, and for $k \geq 0$ in $\mathbb{R}^3$) is verified in an heuristic sense only. More precisely, since the constant $C_0$ involved there is actually unknown, we simply assume $C_0 = 1/2$ and consider a partition $\Gamma_{N,\tilde{h}}$ with a meshsize $\tilde{h}_N$ given approximately by the double of $h_N$. The numerical results to be provided in that section will confirm the suitability of this choice.

## 5. A posteriori error analysis

In this section we derive a reliable and efficient residual based a posteriori error estimator for (4.1). For simplicity, we restrict our analysis to the two-dimensional case with $k = 0$, which means that throughout this section our finite element subspaces $\boldsymbol{H}_h$, $Q_h^p$, and $Q_h^\lambda$ are given by (4.9) (with $k = 0$), (4.10) (with $k = 0$), and (4.13), respectively. Minor modifications allow us to extend our approach to higher polynomial approximations and to $\mathbb{R}^3$. We begin by introducing several notations. We let $\mathcal{E}_h$ be the set of all edges of the triangulation $\mathcal{T}_h$, and given $T \in \mathcal{T}_h$, we let $\mathcal{E}(T)$ be the set of its edges. Then we write $\mathcal{E}_h = \mathcal{E}_h(\Omega) \cup \mathcal{E}_h(\Gamma_D) \cup \mathcal{E}_h(\Gamma_N)$, where $\mathcal{E}_h(\Omega) := \{e \in \mathcal{E}_h : e \subseteq \Omega\}$, $\mathcal{E}_h(\Gamma_D) := \{e \in \mathcal{E}_h : e \subseteq \Gamma_D\}$, and analogously for $\mathcal{E}_h(\Gamma_N)$. In what follows, $h_e$ stands for the length of a given edge $e$. Also, for each edge $e \in \mathcal{E}_h$ we fix a unit normal vector $\boldsymbol{\nu}_e := (\nu_1, \nu_2)^{\mathtt{t}}$, and let $\boldsymbol{s}_e := (-\nu_2, \nu_1)^{\mathtt{t}}$ be the corresponding fixed unit tangential vector along $e$. However, when no confusion arises, we simple write $\boldsymbol{\nu}$ and $\boldsymbol{s}$ instead of $\boldsymbol{\nu}_e$ and $\boldsymbol{s}_e$, respectively. Now, let $\boldsymbol{v} \in \boldsymbol{L}^2(\Omega)$ such that $\boldsymbol{v}|_T \in \boldsymbol{C}(T)$ on each $T \in \mathcal{T}_h$. Hereafter, $\boldsymbol{C}(T)$ denotes $[C(T)]^2$, where $C(T)$ is the space of continuous scalar functions defined on $T$. Then, given

Licensed to University of Oxford. Prepared on Fri Oct 16 07:02:22 EDT 2015 for download from IP 129.67.185.217.
License or copyright restrictions may apply to redistribution; see http://www.ams.org/journal-terms-of-use

$T \in \mathcal{T}_h$ and $e \in \mathcal{E}(T) \cap \mathcal{E}_h(\Omega)$, we denote by $[\boldsymbol{v} \cdot \boldsymbol{s}]$ the tangential jump of $\boldsymbol{v}$ across $e$, that is, $[\boldsymbol{v} \cdot \boldsymbol{s}] := (\boldsymbol{v}|_T - \boldsymbol{v}|_{T'})|_e \cdot \boldsymbol{s}$, where $T$ and $T'$ are the triangles of $\mathcal{T}_h$ having $e$ as a common edge. Similar definitions hold for the tangential jumps of scalar fields $\varphi \in L^2(\Omega)$ such that $\varphi|_T \in C(T)$ on each $T \in \mathcal{T}_h$. Finally, given scalar and vector valued fields $\varphi$ and $\boldsymbol{v} := (v_1, v_2)^{\mathtt{t}}$, respectively, we let

$$\mathbf{curl}\, \varphi := \begin{pmatrix} \frac{\partial \varphi}{\partial x_2} \\ -\frac{\partial \varphi}{\partial x_1} \end{pmatrix} \qquad \text{and} \qquad \mathrm{curl}(\boldsymbol{v}) := \frac{\partial v_2}{\partial x_1} - \frac{\partial v_1}{\partial x_2}\,.$$

Next, letting $(\boldsymbol{u}_h, (p_h, \lambda_h)) \in \boldsymbol{H}_h \times \boldsymbol{Q}_h$ be the unique solution of (4.1), we denote

$$\mathbf{r}(\boldsymbol{u}_h, p_h; \boldsymbol{f}) := \gamma\, \boldsymbol{f} + \gamma\, p_h\, \boldsymbol{f} - \alpha_0\, \gamma\, \boldsymbol{u}_h \quad \text{in} \quad \Omega\,, \tag{5.1}$$

and define for each $T \in \mathcal{T}_h$ the a posteriori error indicator:

$$\begin{aligned} \theta_T^2 := \; & \|\mathrm{div}\, \boldsymbol{u}_h\|_{0,T}^2 + h_T^2\, \|\mathbf{r}(\boldsymbol{u}_h, p_h; \boldsymbol{f})\|_{0,T}^2 \\ & + h_T^2\, \|\mathrm{curl}\big\{\mathbf{r}(\boldsymbol{u}_h, p_h; \boldsymbol{f})\big\}\|_{0,T}^2 \\ & + \sum_{e \in \mathcal{E}(T) \cap \mathcal{E}_h(\Omega)} h_e\, \|[\mathbf{r}(\boldsymbol{u}_h, p_h; \boldsymbol{f}) \cdot \boldsymbol{s}]\|_{0,e}^2 \\ & + \sum_{e \in \mathcal{E}(T) \cap \mathcal{E}_h(\Gamma_N)} h_e \left\| \mathbf{r}(\boldsymbol{u}_h, p_h; \boldsymbol{f}) \cdot \boldsymbol{s} - \frac{d\lambda_h}{d\boldsymbol{s}} \right\|_{0,e}^2 \\ & + \sum_{e \in \mathcal{E}(T) \cap \mathcal{E}_h(\Gamma_N)} h_e \Big\{ \|\lambda_h + p_h\|_{0,e}^2 + \|g - \boldsymbol{u}_h \cdot \boldsymbol{\nu}\|_{0,e}^2 \Big\} \\ & + \sum_{e \in \mathcal{E}(T) \cap \mathcal{E}_h(\Gamma_D)} h_e\, \|\mathbf{r}(\boldsymbol{u}_h, p_h; \boldsymbol{f}) \cdot \boldsymbol{s}\|_{0,e}^2\,, \end{aligned} \tag{5.2}$$

and introduce the global a posteriori error estimator

$$\boldsymbol{\theta} := \left\{ \sum_{T \in \mathcal{T}_h} \theta_T^2 \right\}^{1/2}.$$

Note here that the inclusion of the expression $\|g - \boldsymbol{u}_h \cdot \boldsymbol{\nu}\|_{0,e}^2$ in the definition of $\theta_T^2$ requires the Neumann datum to be smoother than $H_{00}^{-1/2}(\Gamma_N)$, namely $g \in L^2(\Gamma_N)$.

Then, the following theorem constitutes the main result of this section.

**Theorem 5.1.** *Assume that $\boldsymbol{f} \in \boldsymbol{L}^\infty(\Omega)$, $g \in L^2(\Gamma_N)$, and that they are piecewise polynomials on $\mathcal{T}_h$ and $\Gamma_{N,h}$, respectively, for each $h > 0$. Suppose also, as requested by Theorem* 3.1, (3.22), *and Theorem* 4.1, *that*

$$\|\boldsymbol{f}\|_{\infty,\Omega} \leq \frac{1}{2\,\gamma}\, \min\left\{ \frac{1}{\widetilde{C}}, \frac{1}{\widehat{C}} \right\},$$

*and let $(\boldsymbol{u}, (p, \lambda)) \in \boldsymbol{H} \times \boldsymbol{Q}$ and $(\boldsymbol{u}_h, (p_h, \lambda_h)) \in \boldsymbol{H}_h \times \boldsymbol{Q}_h$ be the unique solutions of* (3.1) *and* (4.1), *respectively. Then, there exist constants $C_{\mathtt{rel}} > 0$ and $C_{\mathtt{eff}} > 0$, independent of $h$, such that*

$$C_{\mathtt{eff}}\, \boldsymbol{\theta} \leq \|(\boldsymbol{u}, (p, \lambda)) - (\boldsymbol{u}_h, (p_h, \lambda_h))\|_{\boldsymbol{H} \times \boldsymbol{Q}} \leq C_{\mathtt{rel}}\, \boldsymbol{\theta}\,. \tag{5.3}$$

We remark that when $\boldsymbol{f}$ and $g$ are not both piecewise polynomials, then additional higher order terms (h.o.t.) arising from suitable polynomial approximations of these functions will appear in (5.3). Now, the reliability and efficiency estimates,

Licensed to University of Oxford. Prepared on Fri Oct 16 07:02:22 EDT 2015 for download from IP 129.67.185.217.
License or copyright restrictions may apply to redistribution; see http://www.ams.org/journal-terms-of-use

that is, the upper and lower bounds in (5.3), are derived below in Sections 5.2 and 5.3, respectively. To this end, we first provide some preliminary results.

5.1. **Preliminary results.** In this section we provide several useful results concerning the Clément and Raviart-Thomas interpolation operators, and the Helmholtz decomposition of vector fields in $\boldsymbol{H}(\mathrm{div};\Omega)$.

5.1.1. *Clément interpolator.* Let $I_h : H^1(\Omega) \to X_h$ be the Clément interpolation operator (cf. [20]), where

$$X_h := \left\{ \varphi_h \in C(\bar{\Omega}) : \quad \varphi_h|_T \in P_1(T) \quad \forall\, T \in \mathcal{T}_h \right\}.$$

The local approximation properties of $I_h$ are summarized in the following lemma.

**Lemma 5.2.** *There exist $c_1$, $c_2 > 0$, independent of $h$, such that for all $\varphi \in H^1(\Omega)$ there holds*

$$\|\varphi - I_h(\varphi)\|_{0,T} \leq c_1\, h_T\, \|\varphi\|_{1,\Delta(T)} \qquad \forall\, T \in \mathcal{T}_h$$

*and*

$$\|\varphi - I_h(\varphi)\|_{0,e} \leq c_2\, h_e^{1/2}\, \|\varphi\|_{1,\Delta(e)} \qquad \forall\, e \in \mathcal{E}_h(\Omega) \cup \mathcal{E}_h(\Gamma)\,,$$

*where $\Delta(T) := \bigcup\{T' \in \mathcal{T}_h : T' \cap T \neq \emptyset\}$ and $\Delta(e) := \bigcup\{T' \in \mathcal{T}_h : T' \cap e \neq \emptyset\}$.*

*Proof.* See [20]. □

5.1.2. *Helmholtz decomposition.*

**Lemma 5.3.** *For each $\boldsymbol{v} \in \boldsymbol{H}(\mathrm{div};\Omega)$ there exist $\boldsymbol{\zeta} \in \boldsymbol{H}^1(\Omega)$ and $\varphi \in H^1(\Omega)$, with $\int_\Omega \varphi = 0$, such that $\boldsymbol{v} = \boldsymbol{\zeta} + \mathbf{curl}\,\varphi$ in $\Omega$ and*

$$\|\boldsymbol{\zeta}\|_{1,\Omega} + \|\varphi\|_{1,\Omega} \leq C\, \|\boldsymbol{v}\|_{\mathrm{div},\Omega}\,, \tag{5.4}$$

*where $C$ is a positive constant independent of $\boldsymbol{v}$.*

*Proof.* The proof proceeds as in [24, Lemma 3.4] (see also [29, Section 3.2.2]). □

5.1.3. *Raviart-Thomas interpolator.* Let $\Pi_h : \boldsymbol{H}^1(\Omega) \to \boldsymbol{H}_h$ be the usual Raviart-Thomas interpolation operator, which is characterized by the identity

$$\int_e \Pi_h(\boldsymbol{w}) \cdot \boldsymbol{\nu} = \int_e \boldsymbol{w} \cdot \boldsymbol{\nu} \qquad \forall\, e \in \mathcal{E}_h\,, \quad \forall\, \boldsymbol{w} \in \boldsymbol{H}^1(\Omega)\,. \tag{5.5}$$

It is easy to show, using (5.5), that

$$\mathrm{div}(\Pi_h(\boldsymbol{w})) = \mathcal{P}_h(\mathrm{div}\,\boldsymbol{w}) \qquad \forall\, \boldsymbol{w} \in \boldsymbol{H}^1(\Omega)\,, \tag{5.6}$$

where $\mathcal{P}_h$ is the $L^2(\Omega)$-orthogonal projector onto $Q_h^p$ (cf. (4.10)).

**Lemma 5.4.** *$\Pi_h$ satisfies the following approximation properties,*

$$\|\boldsymbol{w} - \Pi_h(\boldsymbol{w})\|_{0,T} \leq C\, h_T\, \|\boldsymbol{w}\|_{1,T} \quad \forall\, T \in \mathcal{T}_h\,, \quad \forall\, \boldsymbol{w} \in \boldsymbol{H}^1(\Omega) \tag{5.7}$$

*and*

$$\|(\boldsymbol{w} - \Pi_h(\boldsymbol{w})) \cdot \boldsymbol{\nu}\|_{0,e} \leq C\, h_e^{1/2}\, \|\boldsymbol{w}\|_{1,T_e} \quad \forall\, e \in \mathcal{E}_h \cap \partial T_e, \quad \forall\, \boldsymbol{w} \in \boldsymbol{H}^1(\Omega)\,, \tag{5.8}$$

*where $T_e$ in (5.8) is a triangle of $\mathcal{T}_h$ containing $e$ on its boundary.*

*Proof.* See, e.g., [15], [27, Lemmas 3.16 and 3.18], and [49]. □

Licensed to University of Oxford. Prepared on Fri Oct 16 07:02:22 EDT 2015 for download from IP 129.67.185.217.
License or copyright restrictions may apply to redistribution; see http://www.ams.org/journal-terms-of-use

5.2. **Reliability of the a posteriori error estimator.** We first rely on our continuous variational formulation (rewritten as (3.5)–(3.6)) and the associated continuous dependence estimate (3.22). In fact, assuming certainly that $\|\boldsymbol{f}\|_{\infty,\Omega} \leq \frac{1}{2\,\tilde{C}\,\gamma}$, it is easy to show that (3.22) is equivalent to the global inf-sup condition

$$\begin{aligned} &\frac{1}{4\,\tilde{C}}\,\|(\boldsymbol{w},(r,\eta))\|_{\boldsymbol{H}\times\boldsymbol{Q}} \\ &\qquad \leq \sup_{\substack{(\boldsymbol{v},(q,\xi))\in\boldsymbol{H}\times\boldsymbol{Q}\\ (\boldsymbol{v},(q,\xi))\neq 0}} \left\{ \frac{\boldsymbol{a}(\boldsymbol{w},\boldsymbol{v}) + \boldsymbol{b}_1(\boldsymbol{v},(r,\eta)) + \boldsymbol{b}_2(\boldsymbol{w},(q,\xi))}{\|(\boldsymbol{v},(q,\xi))\|_{\boldsymbol{H}\times\boldsymbol{Q}}} \right\}, \end{aligned} \tag{5.9}$$

for all $(\boldsymbol{w},(r,\eta)) \in \boldsymbol{H}\times\boldsymbol{Q}$. Hence, we have the following preliminary estimate for the error.

**Lemma 5.5.** *Let $(\boldsymbol{u},(p,\lambda)) \in \boldsymbol{H}\times\boldsymbol{Q}$ and $(\boldsymbol{u}_h,(p_h,\lambda_h)) \in \boldsymbol{H}_h\times\boldsymbol{Q}_h$ be the unique solutions of (3.1) and (4.1), respectively. Then, there exists a constant $C>0$, independent of $h$, such that*

$$\|(\boldsymbol{u},(p,\lambda))-(\boldsymbol{u}_h,(p_h,\lambda_h))\|_{\boldsymbol{H}\times\boldsymbol{Q}} \leq C\left\{\|\boldsymbol{E}\|_{\boldsymbol{H}'}+\|g-\boldsymbol{u}_h\cdot\boldsymbol{\nu}\|_{0;-1/2,\Gamma_N}+\|\mathrm{div}\,\boldsymbol{u}_h\|_{0,\Omega}\right\},$$

*where $\boldsymbol{E}\in\boldsymbol{H}'$ is an operator defined by*

$$\boldsymbol{E}(\boldsymbol{v}) := \boldsymbol{F}(\boldsymbol{v}) - \boldsymbol{a}(\boldsymbol{u}_h,\boldsymbol{v}) - \boldsymbol{b}_1(\boldsymbol{v},(p_h,\lambda_h)) \qquad \forall\,\boldsymbol{v}\in\boldsymbol{H}\,, \tag{5.10}$$

*and satisfies $\boldsymbol{E}(\boldsymbol{v}_h)=0 \quad \forall\,\boldsymbol{v}_h\in\boldsymbol{H}_h$.*

*Proof.* The first part of the proof follows by applying (5.9) to the error $(\boldsymbol{w},(r,\eta)) := (\boldsymbol{u},(p,\lambda_h))-(\boldsymbol{u}_h,(p_h,\lambda_h))$. In turn, it is clear from the first equation of (4.1) that $\boldsymbol{E}(\boldsymbol{v}_h)=0 \quad \forall\,\boldsymbol{v}_h\in\boldsymbol{H}_h$. □

In order to complete the derivation of the a posteriori error estimate, we need to obtain suitable upper bounds for $\|\boldsymbol{E}\|_{\boldsymbol{H}'}$ and for the Neumann residual $\|g-\boldsymbol{u}_h\cdot\boldsymbol{\nu}\|_{0;-1/2,\Gamma_N}$. We proceed first with the norm of the functional $\boldsymbol{E}$, for which we make use in what follows of the Helmholtz decomposition and the Clément and Raviart-Thomas interpolation operators introduced in Section 5.1 . More precisely, given $\boldsymbol{v}\in\boldsymbol{H}$, we know from Lemma 5.3 that there exist $\boldsymbol{\zeta}\in\boldsymbol{H}^1(\Omega)$ and $\varphi\in H^1(\Omega)$, such that $\boldsymbol{v}=\boldsymbol{\zeta}+\mathbf{curl}\,\varphi$ in $\Omega$ and

$$\|\boldsymbol{\zeta}\|_{1,\Omega} + \|\varphi\|_{1,\Omega} \leq C\,\|\boldsymbol{v}\|_{\mathrm{div},\Omega}\,. \tag{5.11}$$

Hence, we let $\varphi_h := I_h(\varphi)$ and introduce what we call the discrete Helmholtz decomposition

$$\boldsymbol{v}_h := \Pi_h(\boldsymbol{\zeta}) + \mathbf{curl}\,\varphi_h\,,$$

which clearly belongs to $\boldsymbol{H}_h$. In this way, and recalling from Lemma 5.5 that $\boldsymbol{E}(\boldsymbol{v}_h)=0$, we can write

$$\boldsymbol{E}(\boldsymbol{v}) = \boldsymbol{E}(\boldsymbol{v}-\boldsymbol{v}_h) = \boldsymbol{E}\big(\boldsymbol{\zeta}-\Pi_h(\boldsymbol{\zeta})\big) + \boldsymbol{E}\big(\mathbf{curl}(\varphi-\varphi_h)\big)\,, \tag{5.12}$$

where, according to (5.10), the definitions of $\boldsymbol{F}$, $\boldsymbol{a}$, and $\boldsymbol{b}$ (cf. (3.7) and (3.2)), and (5.1), we have

$$\boldsymbol{E}(\boldsymbol{w}) = \int_\Omega \mathbf{r}(\boldsymbol{u}_h,p_h;\boldsymbol{f})\cdot\boldsymbol{w} - \int_\Omega p_h\,\mathrm{div}\,\boldsymbol{w} - \langle\boldsymbol{w}\cdot\boldsymbol{\nu},\lambda_h\rangle_{\Gamma_N} \qquad \forall\,\boldsymbol{w}\in\boldsymbol{H}\,. \tag{5.13}$$

Licensed to University of Oxford. Prepared on Fri Oct 16 07:02:22 EDT 2015 for download from IP 129.67.185.217.
License or copyright restrictions may apply to redistribution; see http://www.ams.org/journal-terms-of-use

Hence, using (5.6), the fact that $p_h|_e \in P_0(e)$ for each $e \in \mathcal{E}_h(\Gamma_N)$, (5.5), and the obvious identity $\mathrm{div}\big\{\mathbf{curl}(\varphi - \varphi_h)\big\} = 0$, we deduce from (5.13) that

$$\boldsymbol{E}\big(\boldsymbol{\zeta}-\Pi_h(\boldsymbol{\zeta})\big) \,=\, \int_\Omega \mathbf{r}(\boldsymbol{u}_h, p_h; \boldsymbol{f})\cdot\big(\boldsymbol{\zeta}-\Pi_h(\boldsymbol{\zeta})\big) - \langle\big(\boldsymbol{\zeta}-\Pi_h(\boldsymbol{\zeta})\big)\cdot\boldsymbol{\nu}, \lambda_h+p_h\rangle_{\Gamma_N}, \tag{5.14}$$

$$\begin{aligned}\boldsymbol{E}\big(\mathbf{curl}(\varphi - \varphi_h)\big) = \int_\Omega \mathbf{r}(\boldsymbol{u}_h, p_h; \boldsymbol{f}) \cdot \mathbf{curl}(\varphi - \varphi_h) \\ - \,\langle\big(\mathbf{curl}(\varphi - \varphi_h)\big) \cdot \boldsymbol{\nu}, \lambda_h\rangle_{\Gamma_N}\,.\end{aligned} \tag{5.15}$$

Consequently, in order to estimate $|\boldsymbol{E}(\boldsymbol{v})|$ in terms of residual terms and $\|\boldsymbol{v}\|_{\boldsymbol{H}}$, we now establish suitable upper bounds for each one of the above two expressions.

**Lemma 5.6.** *There exists $C > 0$, independent of $h$, such that*

$$\big|\boldsymbol{E}\big(\boldsymbol{\zeta} - \Pi_h(\boldsymbol{\zeta})\big)\big| \,\leq\, C\,\left\{\sum_{T\in\mathcal{T}_h} \widetilde{\theta}_T^2\right\}^{1/2} \|\boldsymbol{v}\|_{\boldsymbol{H}}\,, \tag{5.16}$$

*where*

$$\widetilde{\theta}_T^2 \,:=\, h_T^2\,\|\mathbf{r}(\boldsymbol{u}_h, p_h; \boldsymbol{f})\|_{0,T}^2 \,+\, \sum_{e\in\mathcal{E}(T)\cap\mathcal{E}_h(\Gamma_N)} h_e\,\|\lambda_h + p_h\|_{0,e}^2\,. \tag{5.17}$$

*Proof.* The proof basically follows by employing the Cauchy-Schwarz inequality, the approximation properties (5.7) and (5.8) (cf. Lemma 5.4), and the estimate (5.11). We omit further details. □

**Lemma 5.7.** *There exists $C > 0$, independent of $h$, such that*

$$|\boldsymbol{E}\big(\mathbf{curl}(\varphi - \varphi_h)\big)| \,\leq\, C\,\left\{\sum_{T\in\mathcal{T}_h} \widehat{\theta}_T^2\right\}^{1/2} \|\boldsymbol{v}\|_{\mathrm{div},\Omega}\,, \tag{5.18}$$

*where*

$$\begin{aligned}\widehat{\theta}_T^2 :=\, & h_T^2\,\|\mathrm{curl}\big\{\mathbf{r}(\boldsymbol{u}_h, p_h; \boldsymbol{f})\big\}\|_{0,T}^2 \\ & + \sum_{e\in\mathcal{E}(T)\cap\mathcal{E}_h(\Omega)} h_e\,\|[\mathbf{r}(\boldsymbol{u}_h, p_h; \boldsymbol{f})\cdot\boldsymbol{s}]\|_{0,e}^2 \\ & + \sum_{e\in\mathcal{E}(T)\cap\mathcal{E}_h(\Gamma_N)} h_e\,\left\|\mathbf{r}(\boldsymbol{u}_h, p_h; \boldsymbol{f})\cdot\boldsymbol{s} - \frac{d\lambda_h}{d\boldsymbol{s}}\right\|_{0,e}^2 \\ & + \sum_{e\in\mathcal{E}(T)\cap\mathcal{E}_h(\Gamma_D)} h_e\,\|\mathbf{r}(\boldsymbol{u}_h, p_h; \boldsymbol{f})\cdot\boldsymbol{s}\|_{0,e}^2\,.\end{aligned} \tag{5.19}$$

*Proof.* The main tools of this proof include integration by parts, Cauchy-Schwarz inequality, the approximation properties of the Clément interpolator (cf. Lemma 5.2), the fact that the number of elements of $\Delta(T)$ and $\Delta(e)$ are bounded independently of $T \in \mathcal{T}_h$ and $e \in \mathcal{E}_h(\Omega)\cup\mathcal{E}_h(\Gamma_D)\cup\mathcal{E}_h(\Gamma_N)$, respectively, and finally Lemma 5.3. □

Licensed to University of Oxford. Prepared on Fri Oct 16 07:02:22 EDT 2015 for download from IP 129.67.185.217.
License or copyright restrictions may apply to redistribution; see http://www.ams.org/journal-terms-of-use

As a straightforward consequence of identity (5.12) and Lemmas 5.6 and 5.7, we deduce the following upper bound for $\|\boldsymbol{E}\|_{\boldsymbol{H}'}$.

**Lemma 5.8.** *There exists $C > 0$, independent of $h$, such that*

$$\|\boldsymbol{E}\|_{\boldsymbol{H}'} \,\leq\, \left\{ \sum_{T \in \mathcal{T}_h} \left\{ \widetilde{\theta}_T^2 \,+\, \widehat{\theta}_T^2 \right\} \right\}^{1/2} ,$$

*where $\widetilde{\theta}_T^2$ and $\widehat{\theta}_T^2$ are given by* (5.17) *and* (5.19)*, respectively.*

In order to complete the upper bound for $\|(\boldsymbol{u},(p,\lambda)) - (\boldsymbol{u}_h,(p_h,\lambda_h))\|_{\boldsymbol{H}\times\boldsymbol{Q}}$ provided by Lemma 5.5, it only remains to estimate the Neumann residual $\|g - \boldsymbol{u}_h \cdot \boldsymbol{\nu}\|_{0;-1/2,\Gamma_N}$. For this purpose, we now assume that $g \in L^2(\Gamma_N)$, which certainly yields $g - \boldsymbol{u}_h \cdot \boldsymbol{\nu} \in L^2(\Gamma_N)$. Hence, taking $q_h = 0$ in the second equation of (4.1), we get

$$\langle g - \boldsymbol{u}_h \cdot \boldsymbol{\nu}, \xi_h \rangle_{\Gamma_N} \,=\, 0 \qquad \forall\, \xi_h \in Q_h^\lambda \,,$$

which says that $g - \boldsymbol{u}_h \cdot \boldsymbol{\nu}$ is $L^2(\Gamma_N)$-orthogonal to $Q_h^\lambda$ (cf. (4.13)), the continuous piecewise linear functions on the double partition $\Gamma_{N,2h}$ of $\Gamma_N$. Consequently, applying [16, Theorem 2 and eq. (1.4)] and observing that $\Gamma_{N,h}$ and $\Gamma_{N,2h}$ are of bounded variation (which follows from the shape-regularity of $\{\mathcal{T}_h\}_{h>0}$), we obtain

$$\|g - \boldsymbol{u}_h \cdot \boldsymbol{\nu}\|^2_{0;-1/2,\Gamma_N} \,\leq\, c \sum_{e \in \mathcal{E}_h(\Gamma_N)} h_e \, \|g - \boldsymbol{u}_h \cdot \boldsymbol{\nu}\|^2_{0,e} \,. \tag{5.20}$$

Finally, our reliability estimate for $\boldsymbol{\theta}$ (cf. upper bound in (5.3)) follows straightforwardly from Lemmas 5.5 and 5.8, and (5.20).

5.3. **Efficiency of the a posteriori error estimator.** In this section we show the efficiency of our a posteriori error estimator $\boldsymbol{\theta}$. In other words, we provide upper bounds depending on the actual errors for the eight terms defining the local indicator $\theta_T^2$ (cf. (5.2)). The easiest one is the first term, for which, thanks to the incompressibility condition $\operatorname{div} \boldsymbol{u} = 0$ in $\Omega$ (cf. Theorem 3.2), there holds

$$\|\operatorname{div} \boldsymbol{u}_h\|_{0,T} \,=\, \|\operatorname{div}(\boldsymbol{u}_h - \boldsymbol{u})\|_{0,T} \,\leq\, \|\boldsymbol{u} - \boldsymbol{u}_h\|_{\operatorname{div},T} \,. \tag{5.21}$$

The derivation of the corresponding upper bounds for the remaining terms in (5.2) is performed next. To this end, we proceed as in [17] and [28], and apply the localization technique based on triangle-bubble and edge-bubble functions, together with extension operators, discrete trace and inverse inequalities. Therefore, we now introduce further notations and preliminary results. Given $T \in \mathcal{T}_h$ and $e \in \mathcal{E}(T)$, we let $\psi_T$ and $\psi_e$ be the usual triangle-bubble and edge-bubble functions, respectively (see [54, eqs. (1.5) and (1.6)]), which satisfy:

i) $\psi_T \in P_{d+1}(T)$, $\psi_T = 0$ on $\partial T$, $\operatorname{supp}(\psi_T) \subseteq T$, and $0 \leq \psi_T \leq 1$ in $T$.
ii) $\psi_e|_T \in P_d(T)$, $\psi_e = 0$ on $\partial T \setminus e$, $\operatorname{supp}(\psi_e) \subseteq w_e := \cup\{T' \in \mathcal{T}_h : \, e \in \mathcal{E}(T')\}$, and $0 \leq \psi_e \leq 1$ in $w_e$.

We also know from [53] that, given $k \in \mathbb{N} \cup \{0\}$, there exists an extension operator $L : C(e) \to C(T)$ that satisfies $L(p) \in P_k(T)$ and $L(p)|_e = p$ for all $p \in P_k(e)$. Additional properties of $\psi_T$, $\psi_e$ and $L$ are collected in [53, Lemma 4.1]. The inverse estimate (cf. [19, Theorem 3.2.6]) and the discrete trace inequality (cf. [1, Theorem 3.10] or [5, eq. (2.4)]) are also employed.

Licensed to University of Oxford. Prepared on Fri Oct 16 07:02:22 EDT 2015 for download from IP 129.67.185.217.
License or copyright restrictions may apply to redistribution; see http://www.ams.org/journal-terms-of-use

In turn, the following lemma, whose proof makes use of [53, Lemma 4.1] and the inverse estimate, will be required for the terms involving $\mathrm{curl}\big\{\mathbf{r}(\boldsymbol{u}_h,p_h;\boldsymbol{f})\big\}$ and the tangential jumps of $\mathbf{r}(\boldsymbol{u}_h,p_h;\boldsymbol{f})$ across the edges of $\mathcal{T}_h$.

**Lemma 5.9.** *Let $\boldsymbol{\rho}_h \in \boldsymbol{L}^2(\Omega)$ be a piecewise polynomial of degree $k \geq 0$ on each $T \in \mathcal{T}_h$, and let $\boldsymbol{\rho} \in \boldsymbol{L}^2(\Omega)$ be such that $\mathrm{curl}(\boldsymbol{\rho}) = 0$ in $\Omega$. Then, there exist $c, \widetilde{c} > 0$, independent of $h$, such that*

$$\|\mathrm{curl}(\boldsymbol{\rho}_h)\|_{0,T} \leq c\, h_T^{-1}\, \|\boldsymbol{\rho}-\boldsymbol{\rho}_h\|_{0,T} \qquad \forall\, T \in \mathcal{T}_h\,, \tag{5.22}$$

$$\|[\boldsymbol{\rho}_h \boldsymbol{s}]\|_{0,e} \leq \widetilde{c}\, h_e^{-1/2}\, \|\boldsymbol{\rho}-\boldsymbol{\rho}_h\|_{0,\omega_e} \qquad \forall\, e \in \mathcal{E}_h(\Omega)\,. \tag{5.23}$$

*Proof.* For the proof of (5.22) we refer to [10, Lemma 4.3], whereas (5.23) is a slight modification of the proof of [10, Lemma 4.4]. We omit further details. □

Furthermore, as announced in the statement of Theorem 5.1, throughout the rest of this section we assume for simplicity that $\boldsymbol{f}$ and $g$ are piecewise polynomials. The assumption on $\boldsymbol{f}$ is required by the next five lemmas in order to guarantee that $\mathbf{r}(\boldsymbol{u}_h,p_h;\boldsymbol{f})$ and all the other residual expressions involving this term become piecewise polynomials as well. In this way, the estimates from [53, Lemma 4.1] and the inverse estimate can be applied to each one of them when deriving the corresponding efficiency estimates. Similarly, the assumption on $g$ insures that $(g - \boldsymbol{u}_h \cdot \boldsymbol{\nu})$ shares the same property, which is needed below in the proof of our last lemma.

We now let $\mathbf{r}(\boldsymbol{u},p;\boldsymbol{f}) := \big(\gamma\,\boldsymbol{f} + \gamma\, p\,\boldsymbol{f} - \alpha_0\,\gamma\,\boldsymbol{u}\big)$ in $\Omega$, and notice from Theorem 3.2 that there holds $\mathbf{r}(\boldsymbol{u},p;\boldsymbol{f}) = -\nabla p$ in $\Omega$. In addition, it is easy to see that

$$\mathbf{r}(\boldsymbol{u},p;\boldsymbol{f}) - \mathbf{r}(\boldsymbol{u}_h,p_h;\boldsymbol{f}) = \gamma\,(p-p_h)\,\boldsymbol{f} - \alpha_0\,\gamma\,(\boldsymbol{u}-\boldsymbol{u}_h)\,,$$

and hence

$$\begin{aligned} &\|\mathbf{r}(\boldsymbol{u},p;\boldsymbol{f}) - \mathbf{r}(\boldsymbol{u}_h,p_h;\boldsymbol{f})\|_{0,T} \\ &\qquad \leq \gamma\,\|\boldsymbol{f}\|_{\infty,\Omega}\,\|p-p_h\|_{0,T} + \alpha_0\,\gamma\,\|\boldsymbol{u}-\boldsymbol{u}_h\|_{0,T} \quad \forall\, T \in \mathcal{T}_h\,. \end{aligned} \tag{5.24}$$

We continue our efficiency analysis with the following lemma.

**Lemma 5.10.** *There exist $C_1$, $C_2 > 0$, independent of $h$, but depending on $\gamma$, $\alpha_0$, and $\|\boldsymbol{f}\|_{\infty,\Omega}$, such that*

$$h_T^2\,\|\mathrm{curl}\big\{\mathbf{r}(\boldsymbol{u}_h,p_h;\boldsymbol{f})\big\}\|_{0,T}^2 \leq C_1\,\Big\{\|p-p_h\|_{0,T}^2 + \|\boldsymbol{u}-\boldsymbol{u}_h\|_{0,T}^2\Big\} \qquad \forall\, T \in \mathcal{T}_h \tag{5.25}$$

*and*

$$h_e\,\|[\mathbf{r}(\boldsymbol{u}_h,p_h;\boldsymbol{f})\cdot\boldsymbol{s}]\|_{0,e}^2 \leq C_2\,\Big\{\|p-p_h\|_{0,\omega_e}^2 + \|\boldsymbol{u}-\boldsymbol{u}_h\|_{0,\omega_e}^2\Big\} \qquad \forall\, e \in \mathcal{E}_h(\Omega)\,.$$

*Proof.* Since $\mathrm{curl}\big\{\mathbf{r}(\boldsymbol{u},p;\boldsymbol{f})\big\} = -\,\mathrm{curl}\,\nabla p = 0$ in $\Omega$, it suffices to apply Lemma 5.9 to $\boldsymbol{\rho} = \mathbf{r}(\boldsymbol{u},p;\boldsymbol{f})$ and $\boldsymbol{\rho}_h = \mathbf{r}(\boldsymbol{u}_h,p_h;\boldsymbol{f})$, and then employ the estimate (5.24). □

The efficiency estimate for the remaining residual term on each $T \in \mathcal{T}_h$ is given next.

**Lemma 5.11.** *There exists $C_3 > 0$, independent of $h$, but depending on $\gamma$, $\alpha_0$, and $\|\boldsymbol{f}\|_{\infty,\Omega}$, such that*

$$h_T^2\,\|\mathbf{r}(\boldsymbol{u}_h,p_h;\boldsymbol{f})\|_{0,T}^2 \leq C\,\Big\{\|p-p_h\|_{0,T}^2 + h_T^2\|\boldsymbol{u}-\boldsymbol{u}_h\|_{0,T}^2\Big\} \qquad \forall\, T \in \mathcal{T}_h\,, \tag{5.26}$$

Licensed to University of Oxford. Prepared on Fri Oct 16 07:02:22 EDT 2015 for download from IP 129.67.185.217.
License or copyright restrictions may apply to redistribution; see http://www.ams.org/journal-terms-of-use

*Proof.* It is similar to the proof of [28, Lemma 20]. It basically employs an estimate from [53, Lemma 4.1], integration by parts, the Cauchy-Schwarz inequality, and the inverse estimate. □

We now provide the estimate for the residual term involving the tangential derivative of $\lambda_h$.

**Lemma 5.12.** *There exists $C_4 > 0$, independent of $h$, but depending on $\gamma$, $\alpha_0$, and $\|\boldsymbol{f}\|_{\infty,\Omega}$, such that*

(5.27)
$$\sum_{e\in\mathcal{E}_h(\Gamma_N)} h_e \left\| \mathbf{r}(\boldsymbol{u}_h, p_h; \boldsymbol{f})\cdot\boldsymbol{s} - \frac{d\lambda_h}{d\boldsymbol{s}} \right\|^2_{0,e} \leq C_4 \left\{ \sum_{e\in\mathcal{E}_h(\Gamma_N)} \left\{ \|\boldsymbol{u}-\boldsymbol{u}_h\|^2_{0,T_e} + \|p-p_h\|^2_{0,T_e} \right\} + \|\lambda_h-\lambda\|^2_{0;1/2,\Gamma_N} \right\},$$

*where, given $e \in \mathcal{E}_h(\Gamma_N)$, $T_e$ is the triangle of $\mathcal{T}_h$ having $e$ as an edge.*

*Proof.* The proof is an adaptation of [28, Lemma 22]. In particular, we first apply an estimate from [53, Lemma 4.1] and integrate by parts, and then we utilize the boundedness of the tangential derivative $\frac{d}{ds} : H^{1/2}_{00}(\Gamma_N) \to H^{-1/2}_{00}(\Gamma_N)$ (cf. [43]), and the inverse estimate $\|\boldsymbol{\gamma}\|_{0;1/2,\Gamma_N} \leq c\, h^{-1/2} \|\boldsymbol{\gamma}\|_{0,\Gamma_N}$ (cf. [8,46]). We omit further details. □

We remark that the estimate provided by the previous lemma is going to be the only nonlocal bound of the present efficiency analysis. Moreover, it is the only one that needs to assume the quasi-uniformity of $\Gamma_{N,h}$. However, it is possible to show that, under an additional regularity assumption on $\lambda$, namely $\lambda|_e \in H^1(e)$ for each $e \in \mathcal{E}_h(\Gamma_N)$, but without requiring any quasi-uniformity condition, a local estimate can be derived.

We now deal with the last term involving the residual $\mathbf{r}(\boldsymbol{u}_h, p_h; \boldsymbol{f})$.

**Lemma 5.13.** *There exists $C_6 > 0$, independent of $h$, but depending on $\gamma$, $\alpha_0$, and $\|\boldsymbol{f}\|_{\infty,\Omega}$, such that for each $e \in \mathcal{E}_h(\Gamma_D)$ there holds*

$$h_e \|\mathbf{r}(\boldsymbol{u}_h, p_h; \boldsymbol{f})\cdot\boldsymbol{s}\|^2_{0,e} \leq C_6 \left\{ \|\boldsymbol{u}-\boldsymbol{u}_h\|^2_{0,T_e} + \|p-p_h\|^2_{0,T_e} \right\}, \tag{5.28}$$

*where $T_e$ is the triangle of $\mathcal{T}_h$ having $e$ as an edge.*

*Proof.* It follows as in the proof of [28, Lemma 21]. Further details are omitted. □

We end our analysis with the upper bounds for the terms involving the trace of $p$ and the Neumann boundary condition on $\Gamma_N$.

**Lemma 5.14.** *There exists $C_7 > 0$, independent of $h$, but depending on $\gamma$, $\alpha_0$, and $\|\boldsymbol{f}\|_{\infty,\Omega}$, such that for each $e \in \mathcal{E}_h(\Gamma_N)$ there holds*

$$h_e \|\lambda_h + p_h\|^2_{0,e} \leq C_7 \left\{ \|p-p_h\|^2_{0,T_e} + h_e \|\lambda-\lambda_h\|^2_{0,e} + h^2_{T_e} \|\boldsymbol{u}-\boldsymbol{u}_h\|^2_{0,T_e} \right\}, \tag{5.29}$$

*where $T_e$ is the triangle having $e$ as an edge.*

Licensed to University of Oxford. Prepared on Fri Oct 16 07:02:22 EDT 2015 for download from IP 129.67.185.217.
License or copyright restrictions may apply to redistribution; see http://www.ams.org/journal-terms-of-use

*Proof.* It is an adaptation of the proof of [28, Lemma 24] in which the discrete trace inequality plays an important role. We omit additional details. □

**Lemma 5.15.** *There exists $C_8 > 0$, independent of $h$, such that for each $e \in \mathcal{E}_h(\Gamma_N)$ there holds*

$$h_e \, \|g - \boldsymbol{u}_h \cdot \boldsymbol{\nu}\|^2_{0,e} \, \leq \, C_8 \left\{ \|\boldsymbol{u} - \boldsymbol{u}_h\|^2_{0,T_e} \, + \, h^2_{T_e} \, \|\mathrm{div}(\boldsymbol{u} - \boldsymbol{u}_h)\|^2_{0,T_e} \right\}, \tag{5.30}$$

*where $T_e$ is the triangle of $\mathcal{T}_h$ having $e$ as an edge.*

*Proof.* It suffices to adapt the proof of [28, Lemma 25]. The main tools are two estimates from [53, Lemma 4.1], Cauchy-Schwarz inequality, and the inverse estimate. □

We end this section by remarking that the efficiency of $\boldsymbol{\theta}$ follows straightforwardly from the estimate (5.21) and Lemmas 5.10–5.15. More precisely, under the aforementioned additional regularity assumption on $\lambda$, there exists $C > 0$, independent of $h$, but depending on $\gamma$, $\alpha_0$, and $\|\boldsymbol{f}\|_{\infty,\Omega}$, such that for each $T \in \mathcal{T}_h$ the following local efficiency estimate holds

$$\begin{aligned}
\theta^2_T \leq C \Bigg\{ & \|\boldsymbol{u} - \boldsymbol{u}_h\|^2_{\mathrm{div},T} + \sum_{e \in \mathcal{E}(T) \cap \mathcal{E}_h(\Omega)} \left\{ \|p - p_h\|^2_{0,\omega_e} + \|\boldsymbol{u} - \boldsymbol{u}_h\|^2_{0,\omega_e} \right\} \\
& + \sum_{e \in \mathcal{E}(T) \cap \mathcal{E}_h(\Gamma_N)} \Big\{ \|\boldsymbol{u} - \boldsymbol{u}_h\|^2_{\mathrm{div},T_e} + \|p - p_h\|^2_{0,T_e} + h_e \|\lambda - \lambda_h\|^2_{0,e} \\
& \qquad + h_e \left\| \frac{d}{d\boldsymbol{s}} (\lambda - \lambda_h) \right\|^2_{0,e} \Big\} \\
& + \sum_{e \in \mathcal{E}(T) \cap \mathcal{E}_h(\Gamma_D)} \left\{ \|\boldsymbol{u} - \boldsymbol{u}_h\|^2_{0,T_e} \, + \, \|p - p_h\|^2_{0,T_e} \right\} \Bigg\}.
\end{aligned}$$

## 6. Numerical results

In this section we present several numerical examples showing the performance of the mixed finite element scheme (4.1), confirming the reliability and efficiency of the a posteriori error estimator $\boldsymbol{\theta}$ derived in Section 5, and illustrating the behavior of the associated adaptive algorithm. We consider the specific finite element subspaces defined in Section 4.2 with $k = 0$. More precisely, we take (4.9), (4.10), and (4.13) in $\mathbb{R}^2$, whereas (4.9), (4.10), and (4.11) are employed in $\mathbb{R}^3$. We begin by introducing additional notations. The variable $N$ stands for the number of degrees of freedom defining the finite element subspaces $\boldsymbol{H}_h$ and $\boldsymbol{Q}_h$ (equivalently, the number of unknowns of (4.1)), and the individual and global errors are denoted by

$$\mathsf{e}(\boldsymbol{u}) \, := \, \|\boldsymbol{u} - \boldsymbol{u}_h\|_{\mathrm{div},\Omega} \, , \quad \mathsf{e}(p) \, := \, \|p - p_h\|_{0,\Omega} \, , \quad \mathsf{e}(\lambda) \, := \, \|\lambda - \lambda_h\|_{0;1/2,\Gamma_N} \, ,$$

$$\text{and} \quad \mathsf{e} \, := \, \left\{ [\mathsf{e}(\boldsymbol{u})]^2 \, + \, [\mathsf{e}(p)]^2 \, + \, [\mathsf{e}(\lambda)]^2 \right\}^{1/2} ,$$

Licensed to University of Oxford. Prepared on Fri Oct 16 07:02:22 EDT 2015 for download from IP 129.67.185.217.
License or copyright restrictions may apply to redistribution; see http://www.ams.org/journal-terms-of-use

where $(\boldsymbol{u},(p,\lambda)) \in \boldsymbol{H}\times\boldsymbol{Q}$ and $(\boldsymbol{u}_h,(p_h,\lambda_h)) \in \boldsymbol{H}_h\times\boldsymbol{Q}_h$ are the unique solutions of (3.1) and (4.1), respectively. Note that, according to the estimates for the interpolation of Sobolev spaces (cf. [40, Appendix B]), $\|\cdot\|_{0;1/2,\Gamma_N}$ can be approximated by $|\cdot|^{1/2}_{1,\Gamma_N}\,\|\cdot\|^{1/2}_{0,\Gamma_N}$. Furthermore, we define the effectivity index

$$\texttt{eff}(\boldsymbol{\theta}) \;:=\; \texttt{e}/\boldsymbol{\theta}\,,$$

and we let $r(\boldsymbol{u})$, $r(p)$, $r(\lambda)$, and $r$ be the experimental rates of convergence given by

$$r(\boldsymbol{u}) := \frac{\log(\texttt{e}(\boldsymbol{u})/\texttt{e}'(\boldsymbol{u}))}{\log(h/h')}, \quad r(p) := \frac{\log(\texttt{e}(p)/\texttt{e}'(p))}{\log(h/h')},$$
$$r(\lambda) := \frac{\log(\texttt{e}(\lambda)/\texttt{e}'(\lambda))}{\log(h/h')}, \qquad r := \frac{\log\left(\texttt{e}/\texttt{e}'\right)}{\log(h/h')},$$

where $h$ and $h'$ denote two consecutive meshsizes with errors $\texttt{e}$ and $\texttt{e}'$, respectively. However, when Algorithm 1 is applied (see details below), the expression $\log(h/h')$ is replaced by $-\frac{1}{2}\log(N/N')$, where $N$ and $N'$ denote the corresponding degrees of freedom of each triangulation. In addition, we denote the postprocessing error associated to the inverse change of variables needed to recover the original pressure field $P$ from $p_h$, and its associated rate as

$$\texttt{e}(P) = \|P+\gamma^{-1}\log(p_h+1)\|_{0,\Omega} \quad \text{and} \quad r(P) := \frac{\log(\texttt{e}(P)/\texttt{e}'(P))}{\log(h/h')}\,.$$

**Algorithm 1** Mesh adaptation procedure

```
Set i = 0 and construct an initial mesh T_{h_0}
for i = 0, ..., i_max do
    Solve the discrete problem (4.1) on the current mesh T_{h_i} using Algorithm 2
    for T ∈ T_{h_i} do
        Compute the error indicator θ_T associated to T using (5.2)
        if θ_T < ϵ or i ≥ i_max then
            break
        else
            continue
        end if
        if θ_T ≥ (3/5) max{θ_L : L ∈ T_{h_i}} then
            Refine T according to the blue-green strategy
        end if
    end for
    Update the mesh T_{h_i} ← T_{h_{i+1}}
end for
```

Following the analysis of the discrete problem, below a classical Picard (fixed point) algorithm is employed to treat (4.1), which ensures linear convergence [36]. The iterations are stopped when the $L^2$-norm of the pressure residual attains a chosen tolerance $\epsilon_{fp}$. The main steps are summarized in Algorithm 2.

Licensed to University of Oxford. Prepared on Fri Oct 16 07:02:22 EDT 2015 for download from IP 129.67.185.217.
License or copyright restrictions may apply to redistribution; see http://www.ams.org/journal-terms-of-use

**Algorithm 2** Fixed point iteration

1: Set a tolerance $\epsilon_{fp}$ and define $\texttt{res}(0) := 2\epsilon_{fp}$
2: Set $j = 0$ and choose an initial guess for the pressure $p_h^0$ satisfying $p_h^0|_{\Gamma_D} = 0$
3: **for** $j = 1, \ldots, j_{\max}$ **do**
4: Solve the discrete problem

$$\begin{aligned} \boldsymbol{a}(\boldsymbol{u}_h^j, \boldsymbol{v}_h) + \boldsymbol{b}(\boldsymbol{v}_h, (p_h^j, \lambda_h^j)) &= \gamma \int_\Omega \left(p_h^{j-1} + 1\right) \boldsymbol{f} \cdot \boldsymbol{v}_h \qquad && \forall\, \boldsymbol{v}_h \in \boldsymbol{H}_h, \\ \boldsymbol{b}(\boldsymbol{u}_h^j, (q_h, \xi_h)) &= \langle g, \xi_h \rangle_{\Gamma_N} && \forall\, (q_h, \xi_h) \in \boldsymbol{Q}_h, \end{aligned} \tag{6.1}$$

5: Compute the pressure residual $\texttt{res}(j) = \|p_h^j - p_h^{j-1}\|_{0,\Omega}$
6: Update the pressure $p_h^{j-1} \leftarrow p_h^j$
7: **if** $\texttt{res}(j) < \epsilon_{fp}$ **or** $j \geq j_{\max}$ **then**
8: break
9: **else**
10: continue
11: **end if**
12: **end for**

In what follows we describe the examples to be considered, where the accuracy is assessed using the manufactured solution approach. In Example 1 we consider the domain $\Omega := (0,1)^2$ with $\Gamma_D = (0,1) \times \{0\}$ and $\Gamma_N = \partial\Omega \setminus \Gamma_D$, and choose $\boldsymbol{f}$ and $g$ so that the exact solutions of (2.1) and (2.2) are given by the smooth functions

$$U = \boldsymbol{u}(x_1, x_2) := \begin{pmatrix} \sin(\pi x_1)\cos(\pi x_2), \\ -\cos(\pi x_1)\sin(\pi x_2) \end{pmatrix}, \quad p(x_1, x_2) := x_1^2 + x_1 x_2,$$
$$\lambda(x_1, x_2) := -p|_{\Gamma_N}, \quad P(x_1, x_2) := -\gamma^{-1}\log(p+1).$$

We set $\alpha_0 = 0.1$, $\gamma = 10$ and study the accuracy of the discretization using piecewise constant approximations for the pressure field, $\mathbf{RT}_0$ approximations for velocities, and piecewise linear approximations for the Lagrange multiplier. Computed errors, convergence rates, effectivity indexes, and number of fixed point iterations to convergence are displayed in the top rows of Table 1. We observe optimal orders of convergence for all quantities and we notice that a fixed point tolerance of $\epsilon_{fp} = 1e-8$ is met, in average, at around twelve Picard iterations. On the bottom part of Table 1 we display the convergence history associated to an implementation of the discrete counterpart of the nonsymmetric equivalent linear problem (3.5). For the former (and for all remaining examples) we employ a conjugate gradient solver, whereas for the latter we use the unsymmetric multifrontal direct solver for sparse matrices (UMFPACK). Since individual errors, effectivity indexes, and convergence rates are almost identical between the two methods, one could choose any of the two approaches. Here we focus on the first one, mainly since it corresponds to the scheme analyzed in the previous sections and its solution consists of solving symmetric systems. Nevertheless, the second one is certainly appealing from the computational viewpoint. For this example we display approximate velocity components, and original and modified pressures obtained on the finest level (using a mesh of 313041 vertices and 626080 elements) in Figure 1.

Licensed to University of Oxford. Prepared on Fri Oct 16 07:02:22 EDT 2015 for download from IP 129.67.185.217.
License or copyright restrictions may apply to redistribution; see http://www.ams.org/journal-terms-of-use

TABLE 1. Example 1: Experimental convergence for the mixed finite element approximation of the Darcy problem (2.2) and postprocessed pressure $P_h = \gamma^{-1}\log(p_h+1)$ on a sequence of uniformly refined triangulations of $\Omega = (0,1)^2$, using a fixed point formulation with symmetric iterations (top) and a linear nonsymmetric formulation (bottom). Here we have considered the parameters $\alpha_0 = 0.1$, $\gamma = 10$.

| $N$ | $h$ | $\mathtt{e}(\boldsymbol{u})$ | $r(\boldsymbol{u})$ | $\mathtt{e}(p)$ | $r(p)$ | $\mathtt{e}(\lambda)$ | $r(\lambda)$ | $\mathtt{e}(P)$ | $r(P)$ | $\mathtt{eff}(\boldsymbol{\theta})$ | iter |
|---|---|---|---|---|---|---|---|---|---|---|---|
| Problem (3.1) solved iteratively via Algorithm 2 | | | | | | | | | | | |
| 11 | 1.414210 | 0.777153 | – | 0.454962 | – | 1.52585 | – | – | – | 0.238183 | 10 |
| 32 | 0.707107 | 0.465914 | 0.539419 | 0.232287 | 0.969840 | 0.759940 | 0.956320 | 0.024021 | – | 0.264271 | 9 |
| 104 | 0.353553 | 0.264449 | 0.817072 | 0.116629 | 0.993975 | 0.042501 | 2.247691 | 0.014861 | 0.692782 | 0.260534 | 10 |
| 368 | 0.176777 | 0.137101 | 0.947764 | 0.058315 | 0.999992 | 0.015887 | 1.419630 | 0.007794 | 0.931046 | 0.253384 | 11 |
| 1376 | 0.088388 | 0.069199 | 0.986393 | 0.029155 | 1.000112 | 0.008627 | 0.880807 | 0.003943 | 0.982878 | 0.250735 | 12 |
| 5312 | 0.044194 | 0.034682 | 0.996562 | 0.014577 | 1.000041 | 0.004781 | 0.851562 | 0.001977 | 0.995583 | 0.249815 | 11 |
| 20864 | 0.022097 | 0.017352 | 0.999138 | 0.007288 | 1.000011 | 0.002578 | 0.891039 | 0.000990 | 0.998306 | 0.249517 | 11 |
| 82688 | 0.011049 | 0.008677 | 0.999784 | 0.003644 | 1.000010 | 0.001352 | 0.930602 | 0.000496 | 0.997220 | 0.249431 | 12 |
| 329216 | 0.005524 | 0.004339 | 0.999946 | 0.001822 | 1.000000 | 0.000696 | 0.958398 | 0.000249 | 0.989965 | 0.249414 | 11 |
| 1313792 | 0.002762 | 0.002169 | 0.999987 | 0.000911 | 1.000000 | 0.000354 | 0.975827 | 0.000128 | 0.961434 | 0.249416 | 11 |
| Linear non-symmetric problem (3.5) | | | | | | | | | | | |
| 11 | 1.414210 | 0.677153 | – | 0.454962 | – | 1.525851 | – | – | – | 0.238183 | 1 |
| 32 | 0.707107 | 0.465914 | 0.539419 | 0.232287 | 0.969840 | 1.059940 | 0.525629 | 0.0240221 | – | 0.264271 | 1 |
| 104 | 0.353553 | 0.264449 | 0.817072 | 0.116629 | 0.993975 | 0.042501 | 4.640351 | 0.0148613 | 0.692794 | 0.260534 | 1 |
| 368 | 0.176777 | 0.137102 | 0.947764 | 0.058315 | 0.999992 | 0.015887 | 1.419632 | 0.0077944 | 0.931050 | 0.253384 | 1 |
| 1376 | 0.088388 | 0.069199 | 0.986393 | 0.029155 | 1.000112 | 0.008627 | 0.880807 | 0.0039436 | 0.982917 | 0.250732 | 1 |
| 5312 | 0.044194 | 0.034682 | 0.996562 | 0.014577 | 1.000041 | 0.004781 | 0.851562 | 0.0019776 | 0.995739 | 0.249815 | 1 |
| 20864 | 0.022097 | 0.017351 | 0.999138 | 0.007289 | 1.000010 | 0.002578 | 0.891039 | 0.0009895 | 0.998933 | 0.249517 | 1 |
| 82688 | 0.011049 | 0.008677 | 0.999784 | 0.003644 | 1.000000 | 0.001352 | 0.930603 | 0.0004948 | 0.999721 | 0.249431 | 1 |
| 329216 | 0.005524 | 0.004339 | 0.999946 | 0.001822 | 1.000000 | 0.000696 | 0.958398 | 0.0002474 | 0.999882 | 0.249414 | 1 |
| 1313792 | 0.002762 | 0.002169 | 0.999987 | 0.000911 | 1.000000 | 0.000353 | 0.975827 | 0.0001237 | 0.999771 | 0.249416 | 1 |

Licensed to University of Oxford. Prepared on Fri Oct 16 07:02:22 EDT 2015 for download from IP 129.67.185.217.
License or copyright restrictions may apply to redistribution; see http://www.ams.org/journal-terms-of-use

Next, Example 2 focuses on the nonconvex *pacman* domain $\Omega = \{(x_1, x_2) \in \mathbb{R}^2 : x_1^2 + x_2^2 \leq 1\} \setminus (0,1)^2$, with boundaries $\Gamma_N = (0,1) \times \{0\} \bigcup \{0\} \times (0,1)$ and $\Gamma_D = \partial\Omega \setminus \Gamma_D$, where the model problems (2.1), (2.2) admit the following exact solutions

$$U = \boldsymbol{u}(x_1, x_2) := \left((x_1 - c)^2 + (x_2 - c)^2\right)^{-1/2} \begin{pmatrix} c - x_2 \\ x_1 - c \end{pmatrix},$$
$$p(x_1, x_2) := \frac{1 - x_1^2 - x_2^2}{(x_1 - c)^2 + (x_2 - c)^2},$$
$$\lambda(x_1, x_2) := -p|_{\Gamma_N}, \quad P(x_1, x_2) := -\gamma^{-1} \log(p + 1),$$

with $c = 0.025$, satisfying the homogeneous boundary condition on $\Gamma_D$. Both pressure and velocity fields exhibit singularities close to the origin. This example is utilized to illustrate the behavior of the adaptive algorithm associated with $\boldsymbol{\theta}$, which is summarized in Algorithm 1 (see [54]). The corresponding error history for a quasi-uniform and an adaptive refinement strategy are reported in Table 2. In both cases we observe that, in comparison with Example 1, more fixed point iterations are needed to achieve the same tolerance. From the first part of the table, one also notices that the iteration count (based on a pressure residual) is largely affected by the presence of singularities. We also observe a hindered convergence, particularly of the Lagrange multiplier (in comparison with that of the previous example) as well as a much lower and oscillating effectivity index. These anomalies are amended by the adaptive strategy: In the bottom part of Table 2 we observe almost optimal convergence rates for all fields and, for the same fixed point tolerance, an average iteration count closer to the one reported in Table 1. This is also evidenced from Figure 2, where we plot the total error $\mathtt{e}$ versus the degrees of freedom for both refinement strategies and observe suboptimal convergence (approximately of $O(h^{3/4})$) for the quasi-uniform refinement. In addition, snapshots of the adapted meshes at different stages of the algorithm are displayed in Figure 3, exhibiting concentration of the adaptation procedure near the origin, which is the zone of highest gradients and which is well captured by the error estimator. We also show the approximate solutions on the finest level obtained with the same family of finite elements as in the previous example (see Figure 4).

Licensed to University of Oxford. Prepared on Fri Oct 16 07:02:22 EDT 2015 for download from IP 129.67.185.217.
License or copyright restrictions may apply to redistribution; see http://www.ams.org/journal-terms-of-use

TABLE 2. Example 2: Experimental convergence for the mixed finite element approximation of the Darcy problem (2.2) and postprocessed pressure $P_h = \gamma^{-1}\log(p_h+1)$ on a sequence of quasi-uniformly (top) and adaptively (bottom) refined meshes of $\Omega = \{(x_1,x_2)\in\mathbb{R}^2 : x_1^2+x_2^2 \leq 1\}\setminus(0,1)^2$. Here we have considered the parameters $\alpha_0 = 0.1$, $\gamma = 10$.

| $N$ | $h$ | $\mathtt{e}(\boldsymbol{u})$ | $r(\boldsymbol{u})$ | $\mathtt{e}(p)$ | $r(p)$ | $\mathtt{e}(\lambda)$ | $r(\lambda)$ | $\mathtt{e}(P)$ | $r(P)$ | $\mathtt{eff}(\boldsymbol{\theta})$ | iter |
|---|---|---|---|---|---|---|---|---|---|---|---|
| Quasi-uniform refinement | | | | | | | | | | | |
| 225 | 0.396463 | 11.43581 | – | 39.30172 | – | 5.905905 | – | 0.093927 | – | 0.035166 | 33 |
| 675 | 0.234657 | 10.09455 | 0.116705 | 28.75717 | 0.595641 | 3.798687 | 0.757472 | 0.069779 | 0.792872 | 0.018529 | 34 |
| 1625 | 0.153371 | 8.885424 | 0.244053 | 25.28118 | 0.302922 | 2.147508 | 0.661754 | 0.041202 | 0.838860 | 0.016287 | 32 |
| 3530 | 0.102059 | 6.453057 | 0.218888 | 18.87943 | 0.716865 | 1.412040 | 0.529988 | 0.029676 | 0.776951 | 0.013298 | 30 |
| 7960 | 0.068675 | 5.761473 | 0.400416 | 13.89542 | 0.773727 | 0.950806 | 0.873166 | 0.021216 | 0.820906 | 0.026307 | 27 |
| 19930 | 0.043191 | 3.869916 | 0.519673 | 9.780521 | 0.784410 | 0.524016 | 0.816079 | 0.014728 | 0.888218 | 0.009790 | 33 |
| 56730 | 0.025888 | 3.053998 | 0.727651 | 6.672843 | 0.822838 | 0.319769 | 0.729324 | 0.009356 | 0.822051 | 0.007904 | 35 |
| 178440 | 0.014914 | 1.622855 | 1.146492 | 4.555427 | 0.849742 | 0.203720 | 0.866195 | 0.006388 | 0.644759 | 0.068482 | 32 |
| 618660 | 0.008210 | 1.063797 | 0.698373 | 2.461297 | 0.796696 | 0.123352 | 0.711992 | 0.004243 | 0.477433 | 0.016053 | 34 |
| Adaptive refinement | | | | | | | | | | | |
| 861 | 0.210978 | 5.282240 | – | 38.54491 | – | 5.709012 | – | 0.070252 | – | 0.766485 | 13 |
| 1247 | 0.163169 | 3.171521 | 1.073922 | 19.82960 | 1.136872 | 4.367726 | 0.630054 | 0.045942 | 0.962860 | 0.768496 | 14 |
| 1931 | 0.135411 | 1.751252 | 1.015801 | 9.571121 | 1.033150 | 1.353830 | 0.899916 | 0.036824 | 1.011852 | 0.769635 | 15 |
| 3401 | 0.118863 | 0.902784 | 1.038221 | 4.444250 | 1.210593 | 0.869012 | 0.970478 | 0.021465 | 0.955669 | 0.779505 | 13 |
| 6843 | 0.096292 | 0.563009 | 1.052795 | 2.193142 | 1.320374 | 0.613204 | 0.982651 | 0.017271 | 0.940252 | 0.767345 | 14 |
| 17350 | 0.078102 | 0.167351 | 1.092846 | 1.290872 | 1.139381 | 0.391614 | 0.885738 | 0.012131 | 0.948918 | 0.750103 | 16 |
| 46492 | 0.062494 | 0.135441 | 0.930274 | 0.796067 | 0.980809 | 0.234962 | 0.954510 | 0.007226 | 0.958351 | 0.725237 | 13 |
| 127844 | 0.051637 | 0.084252 | 0.950035 | 0.481753 | 0.993065 | 0.172287 | 0.893301 | 0.003629 | 0.963105 | 0.731722 | 14 |
| 329880 | 0.042528 | 0.038337 | 0.989902 | 0.311465 | 0.982892 | 0.123530 | 0.986044 | 0.001995 | 0.953084 | 0.697151 | 13 |
| 783742 | 0.036014 | 0.010492 | 0.978930 | 0.134684 | 0.946813 | 0.101078 | 0.959217 | 0.000642 | 0.930247 | 0.756734 | 14 |

Licensed to University of Oxford. Prepared on Fri Oct 16 07:02:22 EDT 2015 for download from IP 129.67.185.217.
License or copyright restrictions may apply to redistribution; see http://www.ams.org/journal-terms-of-use

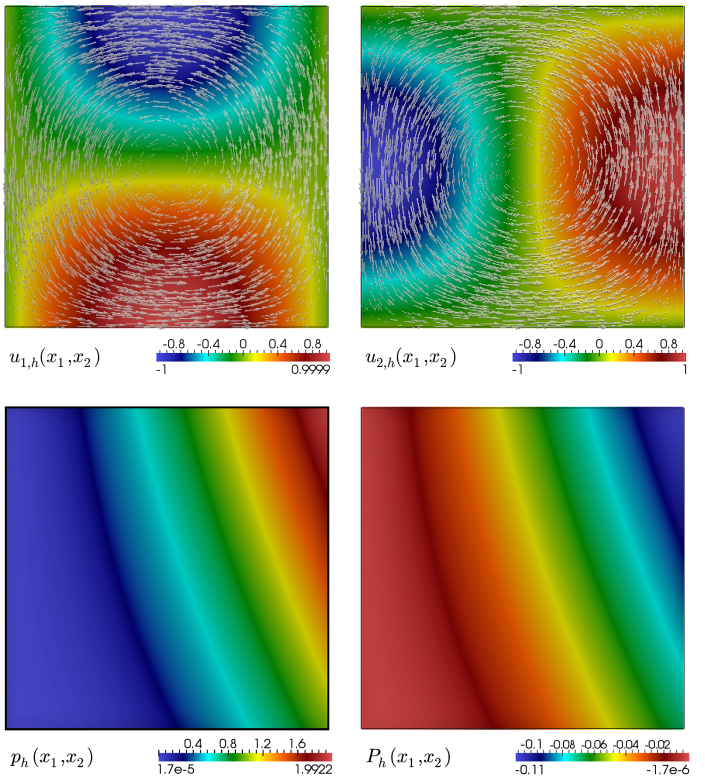


FIGURE 1. Example 1: Approximate velocity components (top), pressure distribution (bottom left), and postprocessed pressure (bottom right), computed using a mesh of 313041 vertices and 626080 elements.

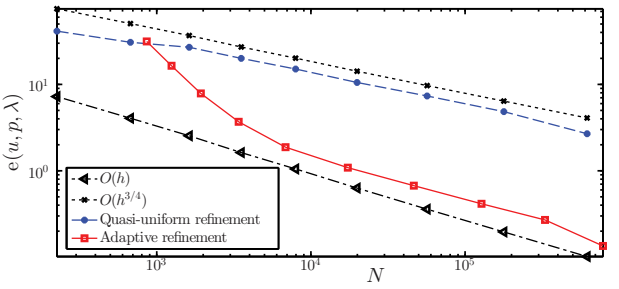


FIGURE 2. Example 2: Decay of the total error with respect to the number of degrees of freedom using a quasi-uniform and an adaptive refinement strategy (see individual errors in Table 2).

Licensed to University of Oxford. Prepared on Fri Oct 16 07:02:22 EDT 2015 for download from IP 129.67.185.217.
License or copyright restrictions may apply to redistribution; see http://www.ams.org/journal-terms-of-use

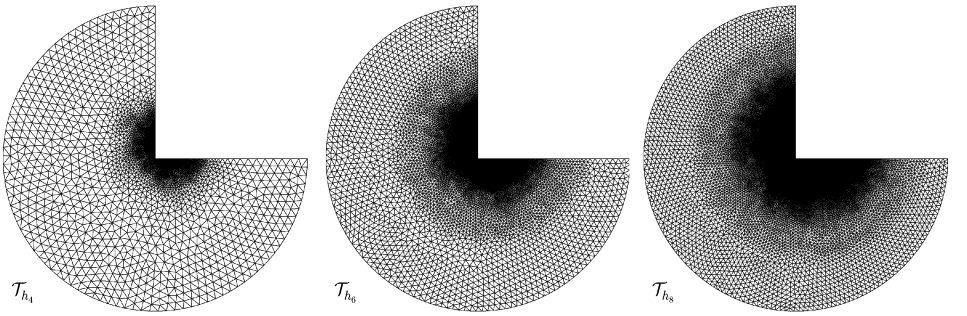


FIGURE 3. Example 2: Adapted meshes after 4,6, and 8 iterations of Algorithm 1.

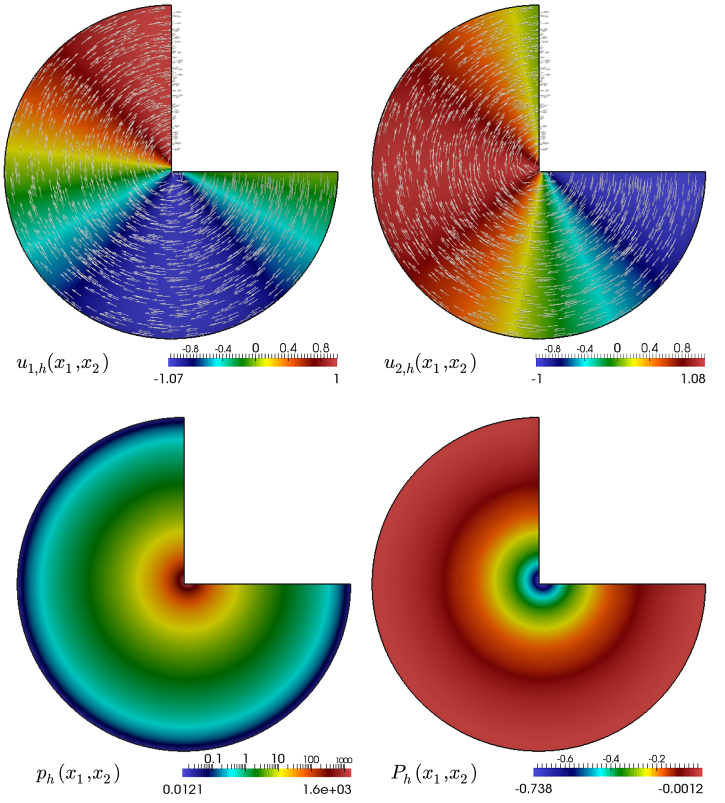


FIGURE 4. Example 2: Approximate velocity components (top), computed pressure distribution (bottom left) and postprocessed pressure (bottom right) obtained on an adapted mesh of 313041 vertices and 626080 elements.

Finally, in Example 3 we illustrate the applicability and accuracy of the proposed numerical method in a three-dimensional scenario. For this we consider $\Omega = (0,1)^3$ where the Dirichlet boundary is the bottom lid of the cube $\Gamma_D = (0,1)\times(0,1)\times\{0\}$,

Licensed to University of Oxford. Prepared on Fri Oct 16 07:02:22 EDT 2015 for download from IP 129.67.185.217.
License or copyright restrictions may apply to redistribution; see http://www.ams.org/journal-terms-of-use

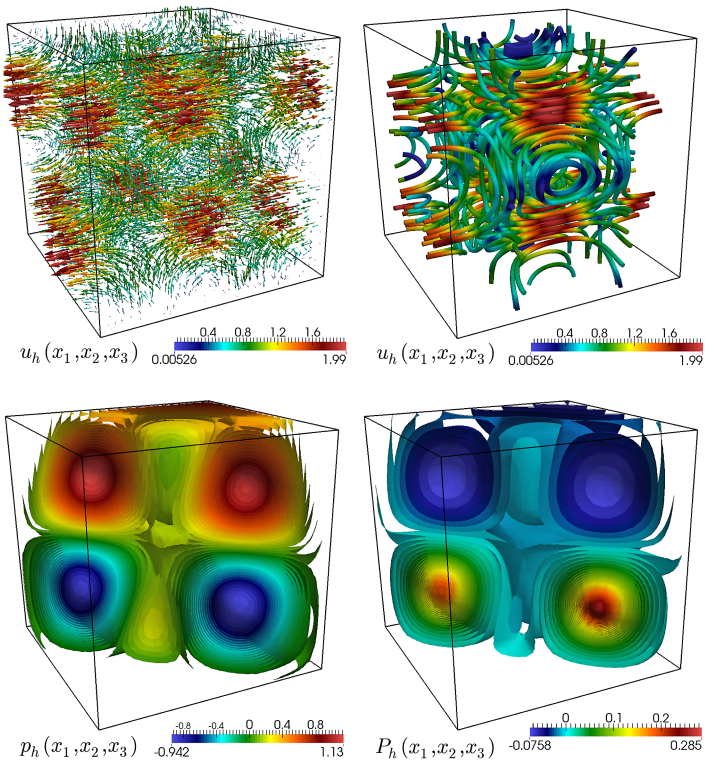


FIGURE 5. Example 3: Approximate velocity vectors and streamlines (top), computed pressure distribution (bottom left) and postprocessed pressure (bottom right) obtained on a uniform mesh of 286906 vertices and 573412 tetrahedral elements.

and the remaining faces constitute the Neumann boundary $\Gamma_N$. We construct $\boldsymbol{f}, g$ so that the exact solutions of the original and auxiliary Darcy problems (2.2), (2.2) are given by

$$
\begin{aligned}
U = \boldsymbol{u}(x_1,x_2,x_3) &:= \begin{pmatrix} \cos(2\pi x_1)\sin(2\pi x_2)\sin(2\pi x_3) \\ \sin(2\pi x_1)\cos(2\pi x_2)\sin(2\pi x_3) \\ -2\sin(2\pi x_1)\sin(2\pi x_2)\cos(2\pi x_3) \end{pmatrix}, \\
p(x_1,x_2,x_3) &:= \sin(2\pi x_1)\sin(2\pi x_2)\sin(2\pi x_3)+x_1x_2x_3, \\
P(x_1,x_2,x_3) &:= -\gamma^{-1}\log(p+1), \\
\lambda(x_1,x_2,x_3) &:= -p|_{\Gamma_N}.
\end{aligned}
$$

As in the preceding tests, we choose the model parameters $\alpha_0 = 0.1$, $\gamma = 10$. Using as a base an initial tetrahedral mesh of 8 vertices and 18 elements, we perform eight successive refinements and we compute experimental errors in different norms. Now we relax the fixed point tolerance to $\epsilon_{fp} = 1e-6$ and observe that the average number of iterations to converge is 14. Optimal rates of convergence are evidenced from Table 3. Approximate velocities and pressure obtained on the finest level (the corresponding mesh has 287496 vertices and 1698450 tetrahedral elements) are presented in Figure 5.

Licensed to University of Oxford. Prepared on Fri Oct 16 07:02:22 EDT 2015 for download from IP 129.67.185.217.
License or copyright restrictions may apply to redistribution; see http://www.ams.org/journal-terms-of-use

TABLE 3. Example 3: Convergence results for the mixed finite element approximation of the Darcy problem (2.2) and postprocessed pressure $P_h = \gamma^{-1}\log(p_h + 1)$ on a sequence of uniformly refined triangulations of $\Omega = (0,1)^3$. Here we have considered the parameters $\alpha_0 = 0.1$, $\gamma = 10$.

| $N$ | $h$ | $\mathsf{e}(\boldsymbol{u})$ | $r(\boldsymbol{u})$ | $\mathsf{e}(p)$ | $r(p)$ | $\mathsf{e}(\lambda)$ | $r(\lambda)$ | $\mathsf{e}(P)$ | $r(P)$ | iter |
|---|---|---|---|---|---|---|---|---|---|---|
| 32 | 1.414211 | 2.043353 | – | 0.495995 | – | 1.747510 | – | 0.124762 | – | 16 |
| 195 | 0.707107 | 1.066271 | 0.968334 | 0.273696 | 0.857752 | 0.809612 | 1.152151 | 0.073987 | 0.794381 | 15 |
| 2616 | 0.282843 | 0.519971 | 0.987055 | 0.155025 | 0.620363 | 0.426881 | 0.820118 | 0.029708 | 0.995827 | 15 |
| 19931 | 0.141421 | 0.246593 | 1.076301 | 0.079143 | 0.969966 | 0.259207 | 0.879427 | 0.019232 | 0.627301 | 13 |
| 96000 | 0.083189 | 0.145919 | 0.988807 | 0.046887 | 0.986583 | 0.168196 | 1.086805 | 0.011871 | 0.909225 | 12 |
| 340107 | 0.054392 | 0.095618 | 0.994823 | 0.030734 | 0.994049 | 0.082207 | 1.063027 | 0.007858 | 0.971003 | 11 |
| 974840 | 0.038222 | 0.067251 | 0.997451 | 0.021619 | 0.997142 | 0.041281 | 1.053195 | 0.005544 | 0.988516 | 10 |
| 2397651 | 0.028284 | 0.034231 | 0.999417 | 0.015553 | 0.998497 | 0.021958 | 0.920208 | 0.003473 | 0.983695 | 14 |
| 3256096 | 0.018757 | 0.018630 | 0.988616 | 0.007387 | 0.998462 | 0.011346 | 0.983085 | 0.001824 | 0.886841 | 14 |

Licensed to University of Oxford. Prepared on Fri Oct 16 07:02:22 EDT 2015 for download from IP 129.67.185.217.
License or copyright restrictions may apply to redistribution; see http://www.ams.org/journal-terms-of-use

## References


[1] S. Agmon, *Lectures on elliptic boundary value problems*, Van Nostrand Mathematical Studies, No. 2, D. Van Nostrand Co., Inc., Princeton, NJ, Toronto, London, 1965. MR0178246 (31 #2504)

[2] E. Ahusborde, M. Azaïez, F. Ben Belgacem, and C. Bernardi, *Automatic simplification of Darcy's equations with pressure dependent permeability*, ESAIM Math. Model. Numer. Anal. **47** (2013), no. 6, 1797–1820, DOI 10.1051/m2an/2013089. MR3123377

[3] M. Ainsworth and J. T. Oden, *A posteriori error estimation in finite element analysis*, Comput. Methods Appl. Mech. Engrg. **142** (1997), no. 1-2, 1–88, DOI 10.1016/S0045-7825(96)01107-3. MR1442375 (98e:65092)

[4] A. Alonso, *Error estimators for a mixed method*, Numer. Math. **74** (1996), no. 4, 385–395, DOI 10.1007/s002110050222. MR1414415 (97g:65212)

[5] D. N. Arnold, *An interior penalty finite element method with discontinuous elements*, SIAM J. Numer. Anal. **19** (1982), no. 4, 742–760, DOI 10.1137/0719052. MR664882 (83f:65173)

[6] M. Azaïez, F. Ben Belgacem, C. Bernardi, and N. Chorfi, *Spectral discretization of Darcy's equations with pressure dependent porosity* (English, with English and French summaries), Appl. Math. Comput. **217** (2010), no. 5, 1838–1856, DOI 10.1016/j.amc.2010.06.014. MR2727929 (2011i:76061)

[7] M. Azaïez, F. Ben Belgacem, M. Grundmann, and H. Khallouf, *Staggered grids hybrid-dual spectral element method for second-order elliptic problems. Application to high-order time splitting methods for Navier-Stokes equations*, Comput. Methods Appl. Mech. Engrg. **166** (1998), no. 3-4, 183–199, DOI 10.1016/S0045-7825(98)00069-3. MR1659191 (99j:76070)

[8] I. Babuška and A. K. Aziz, *Survey lectures on the mathematical foundations of the finite element method*, The mathematical foundations of the finite element method with applications to partial differential equations (Proc. Sympos., Univ. Maryland, Baltimore, Md., 1972), Academic Press, New York, 1972, pp. 1–359. With the collaboration of G. Fix and R. B. Kellogg. MR0421106 (54 #9111)

[9] I. Babuška and G. N. Gatica, *On the mixed finite element method with Lagrange multipliers*, Numer. Methods Partial Differential Equations **19** (2003), no. 2, 192–210, DOI 10.1002/num.10040. MR1958060 (2004b:65174)

[10] T. P. Barrios, G. N. Gatica, M. González, and N. Heuer, *A residual based a posteriori error estimator for an augmented mixed finite element method in linear elasticity*, M2AN Math. Model. Numer. Anal. **40** (2006), no. 5, 843–869 (2007), DOI 10.1051/m2an:2006036. MR2293249 (2008b:74039)

[11] Barus, C., *Isotherms, isopiestics and isometrics relative to viscosity.* American Journal of Science, **45** (1893) 87–96.

[12] C. Bernardi, C. Canuto, and Y. Maday, *Generalized inf-sup conditions for Chebyshev spectral approximation of the Stokes problem*, SIAM J. Numer. Anal. **25** (1988), no. 6, 1237–1271, DOI 10.1137/0725070. MR972452 (90e:65151)

[13] C. Bernardi, F. Hecht, and O. Pironneau, *Coupling Darcy and Stokes equations for porous media with cracks*, M2AN Math. Model. Numer. Anal. **39** (2005), no. 1, 7–35, DOI 10.1051/m2an:2005007. MR2136198 (2006a:76107)

[14] D. Braess and R. Verfürth, *A posteriori error estimators for the Raviart-Thomas element*, SIAM J. Numer. Anal. **33** (1996), no. 6, 2431–2444, DOI 10.1137/S0036142994264079. MR1427472 (97m:65201)

[15] F. Brezzi and M. Fortin, *Mixed and Hybrid Finite Element Methods*, Springer Series in Computational Mathematics, vol. 15, Springer-Verlag, New York, 1991. MR1115205 (92d:65187)

[16] C. Carstensen, *An a posteriori error estimate for a first-kind integral equation*, Math. Comp. **66** (1997), no. 217, 139–155, DOI 10.1090/S0025-5718-97-00790-4. MR1372001 (97e:65147)

[17] C. Carstensen, *A posteriori error estimate for the mixed finite element method*, Math. Comp. **66** (1997), no. 218, 465–476, DOI 10.1090/S0025-5718-97-00837-5. MR1408371 (98a:65162)

[18] J. Chang, and K. B. Nakshatrala, *Modification to Darcy model for high pressure and high velocity applications and associated mixed finite element formulations.* arXiv:1306.5216[cs.NA]

[19] P. G. Ciarlet, *The Finite Element Method for Elliptic Problems*, North-Holland Publishing Co., Amsterdam-New York-Oxford, 1978. Studies in Mathematics and its Applications, Vol. 4. MR0520174 (58 #25001)


Licensed to University of Oxford. Prepared on Fri Oct 16 07:02:22 EDT 2015 for download from IP 129.67.185.217.
License or copyright restrictions may apply to redistribution; see http://www.ams.org/journal-terms-of-use

[20] Ph. Clément, *Approximation by finite element functions using local regularization* (English, with Loose French summary), Rev. Française Automat. Informat. Recherche Opérationnelle Sér., RAIRO Analyse Numérique **9** (1975), no. R-2, 77–84. MR0400739 (53 #4569)

[21] M. Daadaa, *Discrétisation Spectrale et par Éléments Spectraux des Équations de Darcy*. Ph.D. Thesis, Université Pierre et Marie Curie, Paris (2009).

[22] H. Darcy, *Les fontaines publiques de la ville de Dijon*. Dalmont, Paris (1856).

[23] M. Discacciati, E. Miglio, and A. Quarteroni, *Mathematical and numerical models for coupling surface and groundwater flows*, Appl. Numer. Math. **43** (2002), no. 1-2, 57–74, DOI 10.1016/S0168-9274(02)00125-3. MR1936102 (2003h:76087)

[24] C. Domínguez, G. N. Gatica, and S. Meddahi, *A posteriori error analysis of a fully-mixed finite element method for a two-dimensional fluid-solid interaction problem*. Preprint 2014-02, Centro de Investigación en Ingeniería Matemática (CI$^2$MA), Universidad de Concepción, Concepción, Chile, (2014).

[25] V. J. Ervin, E. W. Jenkins, and S. Sun, *Coupling nonlinear Stokes and Darcy flow using mortar finite elements*, Appl. Numer. Math. **61** (2011), no. 11, 1198–1222, DOI 10.1016/j.apnum.2011.08.002. MR2842139 (2012j:65398)

[26] J. Galvis and M. Sarkis, *Non-matching mortar discretization analysis for the coupling Stokes-Darcy equations*, Electron. Trans. Numer. Anal. **26** (2007), 350–384. MR2391227 (2009a:76120)

[27] G. N. Gatica, *A Simple Introduction to the Mixed Finite Element Method: Theory and Applications*, Springer Briefs in Mathematics, Springer, Cham, 2014. MR3157367

[28] G. N. Gatica, L. F. Gatica, and A. Márquez, *Analysis of a pseudostress-based mixed finite element method for the Brinkman model of porous media flow*, Numer. Math. **126** (2014), no. 4, 635–677, DOI 10.1007/s00211-013-0577-x. MR3175180

[29] G. N. Gatica, G. C. Hsiao, and S. Meddahi, *A residual-based a posteriori error estimator for a two-dimensional fluid-solid interaction problem*, Numer. Math. **114** (2009), no. 1, 63–106, DOI 10.1007/s00211-009-0250-6. MR2557870 (2011a:65401)

[30] G. N. Gatica and M. Maischak, *A posteriori error estimates for the mixed finite element method with Lagrange multipliers*, Numer. Methods Partial Differential Equations **21** (2005), no. 3, 421–450, DOI 10.1002/num.20050. MR2128589 (2005m:65266)

[31] G. N. Gatica, S. Meddahi, and R. Oyarzúa, *A conforming mixed finite-element method for the coupling of fluid flow with porous media flow*, IMA J. Numer. Anal. **29** (2009), no. 1, 86–108, DOI 10.1093/imanum/drm049. MR2470941 (2010b:76118)

[32] G. N. Gatica, R. Oyarzúa, and F.-J. Sayas, *Analysis of fully-mixed finite element methods for the Stokes-Darcy coupled problem*, Math. Comp. **80** (2011), no. 276, 1911–1948, DOI 10.1090/S0025-5718-2011-02466-X. MR2813344 (2012i:65259)

[33] V. Girault, F. Murat, and A. Salgado, *Finite element discretization of Darcy's equations with pressure dependent porosity*, M2AN Math. Model. Numer. Anal. **44** (2010), no. 6, 1155–1191, DOI 10.1051/m2an/2010019. MR2769053 (2012e:76126)

[34] V. Girault and P.-A. Raviart, *Finite Element Methods for Navier-Stokes Equations*, Springer Series in Computational Mathematics, vol. 5, Springer-Verlag, Berlin, 1986. Theory and algorithms. MR851383 (88b:65129)

[35] V. Girault and M. F. Wheeler, *Numerical discretization of a Darcy-Forchheimer model*, Numer. Math. **110** (2008), no. 2, 161–198, DOI 10.1007/s00211-008-0157-7. MR2425154 (2009g:65163)

[36] O. A. Karakashian, *On a Galerkin-Lagrange multiplier method for the stationary Navier-Stokes equations*, SIAM J. Numer. Anal. **19** (1982), no. 5, 909–923, DOI 10.1137/0719066. MR672567 (83j:65107)

[37] T. Karper, K.-A. Mardal, and R. Winther, *Unified finite element discretizations of coupled Darcy-Stokes flow*, Numer. Methods Partial Differential Equations **25** (2009), no. 2, 311–326, DOI 10.1002/num.20349. MR2483769 (2010a:65240)

[38] J.-L. Lions and E. Magenes, *Problèmes aux Limites non Homogènes et Applications I*. Dunod, Paris, 1968.

[39] A. Márquez, S. Meddahi, and F.-J. Sayas, *Strong coupling of finite element methods for the Stokes-Darcy problem*. IMA Journal of Numerical Analysis (2014) doi: 10.1093/imanum/dru023.

[40] W. McLean, *Strongly Elliptic Systems and Boundary Integral Equations*, Cambridge University Press, Cambridge, 2000. MR1742312 (2001a:35051)

Licensed to University of Oxford. Prepared on Fri Oct 16 07:02:22 EDT 2015 for download from IP 129.67.185.217.
License or copyright restrictions may apply to redistribution; see http://www.ams.org/journal-terms-of-use

[41] K. B. Nakshatrala and K. R. Rajagopal, *A numerical study of fluids with pressure-dependent viscosity flowing through a rigid porous medium*, Internat. J. Numer. Methods Fluids **67** (2011), no. 3, 342–368, DOI 10.1002/fld.2358. MR2835720 (2012g:76171)

[42] K. B. Nakshatrala and D. Z. Turner, *A mixed formulation for a modification to Darcy equation based on Picard linearization and numerical solutions to large-scale realistic problems*, Int. J. Comput. Methods Eng. Sci. Mech. **14** (2013), no. 6, 524–541, DOI 10.1080/15502287.2013.822942. MR3172099

[43] J. Nečas, *Les Méthodes Directes en Théorie des Équations Elliptiques*. Mason, Paris, 1967.

[44] H. Pan and H. Rui, *Mixed element method for two-dimensional Darcy-Forchheimer model*, J. Sci. Comput. **52** (2012), no. 3, 563–587, DOI 10.1007/s10915-011-9558-3. MR2948707

[45] E.-J. Park, *Mixed finite element methods for generalized Forchheimer flow in porous media*, Numer. Methods Partial Differential Equations **21** (2005), no. 2, 213–228, DOI 10.1002/num.20035. MR2114948 (2005i:76075)

[46] S. Prössdorf and B. Silbermann, *Numerical Analysis for Integral and Related Operator Equations*, Mathematische Lehrbücher und Monographien, II. Abteilung: Mathematische Monographien [Mathematical Textbooks and Monographs, Part II: Mathematical Monographs], vol. 84, Akademie-Verlag, Berlin, 1991. MR1206476 (94f:65126a)

[47] K. R. Rajagopal, *On a hierarchy of approximate models for flows of incompressible fluids through porous solids*, Math. Models Methods Appl. Sci. **17** (2007), no. 2, 215–252, DOI 10.1142/S0218202507001899. MR2292356 (2007k:76156)

[48] B. Rivière and I. Yotov, *Locally conservative coupling of Stokes and Darcy flows*, SIAM J. Numer. Anal. **42** (2005), no. 5, 1959–1977, DOI 10.1137/S0036142903427640. MR2139232 (2006a:76035)

[49] J. E. Roberts and J.-M. Thomas, *Mixed and hybrid methods*, Handbook of Numerical Analysis, Vol. II, Handb. Numer. Anal., II, North-Holland, Amsterdam, 1991, pp. 523–639. MR1115239

[50] S. Srinivasan, A. Bonito, and K. R. Rajagopal, *Flow of a fluid through a porous solid due to high pressure gradients*. Journal of Porous Media, **16(3)** (2013) 193–203.

[51] S. Srinivasan and K. R. Rajagopal, *A thermodynamic basis for the derivation of the Darcy, Forchheimer and Brinkman models for flows through porous media and their generalizations*, International Journal of Nonlinear Mechanics, **58** (2014) 162–166.

[52] R. Verfürth, *A posteriori error estimators for the Stokes equations*, Numer. Math. **55** (1989), no. 3, 309–325, DOI 10.1007/BF01390056. MR993474 (90d:65187)

[53] R. Verfürth, *A posteriori error estimation and adaptive mesh-refinement techniques*, J. Comput. Appl. Math. **50** (1994), no. 1-3, 67–83, DOI 10.1016/0377-0427(94)90290-9. MR1284252 (95c:65171)

[54] R. Verfürth, *A Review of A-Posteriori Error Estimation and Adaptive Mesh-Refinement Techniques*, John Wiley and Teubner Series, Advances in Numerical Mathematics 1996.

[55] X. Xie, J. Xu, and G. Xue, *Uniformly-stable finite element methods for Darcy-Stokes-Brinkman models*, J. Comput. Math. **26** (2008), no. 3, 437–455. MR2421892 (2009g:76087)

CI$^2$MA and Departamento de Ingeniería Matemática, Universidad de Concepción, Casilla 160-C, Concepción, Chile

*E-mail address*: ggatica@ci2ma.udec.cl

Institute of Earth Sciences, Quartier UNIL-Mouline, Bâtiment Géopolis, University of Lausanne, CH-1015 Lausanne, Switzerland

*E-mail address*: ricardo.ruizbaier@unil.ch

Mathematical Institute, Faculty of Mathematics and Physics, Charles University in Prague, Prague 8, 186 75, Czech Republic

*E-mail address*: gtierra@karlin.mff.cuni.cz

Licensed to University of Oxford. Prepared on Fri Oct 16 07:02:22 EDT 2015 for download from IP 129.67.185.217.

License or copyright restrictions may apply to redistribution; see http://www.ams.org/journal-terms-of-use